Clustering for epidemics on networks

A geometric approach

Prasse, Bastian; Devriendt, Karel; Van Mieghem, Piet

DOI
10.1063/5.0048779

Publication date
2021

Document Version
Accepted author manuscript

Published in
Chaos

Clustering for epidemics on networks: a geometric approach

Bastian Prasse*, Karel Devriendt† and Piet Van Mieghem*

May 7, 2021

Abstract

Infectious diseases typically spread over a contact network with millions of individuals, whose sheer size is a tremendous challenge to analysing and controlling an epidemic outbreak. For some contact networks, it is possible to group individuals into clusters. A high-level description of the epidemic between a few clusters is considerably simpler than on an individual level. However, to cluster individuals, most studies rely on equitable partitions, a rather restrictive structural property of the contact network. In this work, we focus on Susceptible-Infected-Susceptible (SIS) epidemics, and our contribution is threefold. First, we propose a geometric approach to specify *all* networks for which an epidemic outbreak simplifies to the interaction of only a few clusters. Second, for the complete graph and *any* initial viral state vectors, we derive the closed-form solution of the nonlinear differential equations of the N-Intertwined Mean-Field Approximation (NIMFA) of the SIS process. Third, by relaxing the notion of equitable partitions, we derive low-complexity approximations and bounds for epidemics on *arbitrary* contact networks. Our results are an important step towards understanding and controlling epidemics on large networks.

An infectious diseases spreads from one individual to another only if the two individuals are in contact, e.g., by being closer than 1.5 meters. The specification of all contacts between individuals in a population results in the *contact network*: every individual corresponds to a node, and there is a link between two nodes if the respective individuals are in contact. Since most infectious diseases spread among large populations, the contact network is often of tremendous size, which results in challenging, large-scale epidemic models. To reduce the complexity of such individual-based epidemic models, a common approach is to describe the epidemic, at least approximately, between groups (clusters) of individuals. However, only a few types of contact networks are known to admit a grouping of individuals that yields an accurate, low-complexity description of the epidemic. In this work, we focus on Susceptible-Infected-Susceptible (SIS) epidemics and determine *all* types of contact networks that admit an exact grouping of individuals. Furthermore, for any contact network, we derive low-complexity approximations and bounds of the SIS epidemic model based on grouping individuals.

*Faculty of Electrical Engineering, Mathematics and Computer Science, P.O Box 5031, 2600 GA Delft, The Netherlands; *email*: b.prasse@tudelft.nl, p.f.a.vanmieghem@tudelft.nl

†Mathematical Institute, University of Oxford, OX2 6GG Oxford UK; email: devriendt@maths.ox.ac.uk; Also at Alan Turing Institute, NW1 2DB London, UK

1 Introduction

Modern epidemiology encompasses a broad range of spreading phenomena [35, 31, 22]. The majority of viruses spread through a population of tremendous size, which renders individual-based modelling impractical. However, most applications do not require to model an epidemic on individual level. Instead, a mesoscale description of the epidemic often is sufficient. For instance, suppose the outbreak of a virus is modelled on the level of neighbourhoods. Then, sophisticated lockdown measures can be deployed which constrain neighbourhoods differently, depending on the prevalence of the virus in the respective neighbourhood. The natural way to obtain a mesoscale description of the epidemic is *clustering* (or grouping) of individuals, for instance, by assigning individuals with similar age or location to the same cluster. Thus, all individuals in one cluster are considered indistinguishable and exchangeable. Additionally to the complexity reduction, clustering for epidemics on networks has the advantage that, on a mesoscale description, temporal fluctuations of the individual-based contact network may average out.

We consider a contact network with N nodes. Every node $i = 1, ..., N$ corresponds to an individual or a group of individuals. We focus on the Susceptible-Infected-Susceptible (SIS) epidemic process in an individual-based mean-field approximation, where every node i has a viral state $v_i(t) \in [0, 1]$ at every time t. The evolution of the viral state $v_i(t)$ is governed by a set of N nonlinear differential equations:

Definition 1 (NIMFA [25, 60, 54])**.** *For every node i, the viral state $v_i(t)$ evolves in continuous time $t \geq 0$ as*

$$\frac{dv_i(t)}{dt} = -\delta_i v_i(t) + (1 - v_i(t)) \sum_{j=1}^{N} \beta_{ij} v_j(t), \tag{1}$$

where $\delta_i > 0$ is the curing rate *of node i, and $\beta_{ij} > 0$ is the* infection rate *from node j to i.*

If the nodes correspond to individuals, then the differential equations (1) follow from a mean-field approximation of the stochastic SIS process [60, 57], and the viral state $v_i(t)$ approximates the expected value $\mathrm{E}[X_i(t)]$ of the zero-one state $X_i(t)$ of the stochastic SIS process. For a zero-one, or Bernoulli, random variable the expectation $\mathrm{E}[X_i(t)]$ is equal to the probability $\Pr[X_i(t) = 1]$ that node i is infected at time t. In the remainder of this work, we refer to (1) as NIMFA, which stands for "N-Intertwined Mean-Field Approximation" [60, 57]. The advantage of NIMFA is that the SIS Markov chain with 2^N states is approximated by N nonlinear differential equations. NIMFA follows from the SIS process by the approximation $\mathrm{E}[X_i(t)X_j(t)] \approx \mathrm{E}[X_i(t)]\,\mathrm{E}[X_j(t)]$. Around the epidemic threshold, the approximation of the stochastic SIS process by NIMFA might be inaccurate [60]. Furthermore, we stress that NIMFA (1) assumes that the viral dynamics are Markovian and that the infection rates β_{ij} do not depend on time t. Markovian and non-Markovian viral dynamics can be substantially different [55].

On the other hand, nodes can be interpreted as groups of individuals [25, 34, 23]. Then, the viral state $v_i(t) \in [0, 1]$ is the fraction of infected individuals in node i. For group-based epidemic models, the infection rates β_{ij} are determined by the mobility flow, or diffusion of individuals, between group i and j. For more details on *metapopulation* models, we refer the reader to [8, 9, 23] and [35, Section

IX.]. The results of this work apply to NIMFA (1) for both an individual-based and a metapopulation setting.

The contact network, assumed to be fixed and time-invariant, corresponds to the $N \times N$ infection rate matrix B, which is composed of the elements β_{ij}. We denote by $\mathrm{diag}(x)$ the $N \times N$ diagonal matrix with the vector components of $x \in \mathbb{R}^N$ on its diagonal. We denote the $N \times N$ curing rate matrix $S = \mathrm{diag}(\delta_1, ..., \delta_N)$. Then, the matrix representation of NIMFA (1) is

$$\frac{dv(t)}{dt} = -Sv(t) + \mathrm{diag}\left(u - v(t)\right) Bv(t), \tag{2}$$

where $v(t) = (v_1(t), ..., v_N(t))^T$ is the viral state vector at time t, and u is the $N \times 1$ all-one vector. *Homogeneous* NIMFA [60] assumes the same infection rate β and curing rate δ for all nodes,

$$\frac{dv(t)}{dt} = -\delta v(t) + \beta \mathrm{diag}\left(u - v(t)\right) Av(t), \tag{3}$$

where A is an $N \times N$ zero-one adjacency matrix.

For NIMFA (1), the basic reproduction number R_0 follows [52] as

$$R_0 = \rho(S^{-1}B), \tag{4}$$

where $\rho(M)$ denotes the spectral radius of a square matrix M. Around the *epidemic threshold condition* $R_0 = 1$, there is a bifurcation [25]. If $R_0 \leq 1$, then the all-healthy state, $v_i(t) = 0$ for all nodes i, is the only equilibrium of NIMFA (2), and it holds that $v(t) \to 0$ as $t \to \infty$. If $R_0 > 1$, then there is a second equilibrium, the *steady-state* vector v_∞, with positive components, and it holds that $v(t) \to v_\infty$ as $t \to \infty$, if $v(0) \neq 0$. For homogeneous NIMFA (3), the condition $R_0 > 1$ reduces to $\tau > \tau_c$ with the effective infection rate $\tau = \beta/\delta$ and the epidemic threshold $\tau_c = 1/\rho(A)$, where $\rho(A)$ denotes the spectral radius of the adjacency matrix A.

The contact network, given by the matrix B, has a significant impact on the virus spread [35, 31, 22]. First, the structure of the contact network has an influence on the basic reproduction number R_0. For instance, for homogeneous NIMFA (3) on scale-free networks, the epidemic threshold $\tau_c = 1/\rho(A)$ converges to zero [36] as the number of nodes $N \to \infty$. Hence, there is always a non-zero steady state v_∞ for sufficiently large scale-free networks, regardless of the effective infection rate τ. Second, the contact network determines the steady state $v_{\infty,i}$ of every node i. In particular, the steady-state vector v_∞ can be expressed as a power series [58, 42, 19] in terms of the eigenvectors of the infection rate matrix B. Third, some contact networks give rise to disease localisation [17, 14, 10, 28], which means that the spread of the epidemic is restricted to parts of the networks when the basic reproduction R_0 is just above 1.

Many papers deal with clustering of individuals into *communities* [7, 1, 38], where individuals within the same community are densely connected, and there are only few links between individuals of different communities. Hence, communities are defined by structural properties of the contact graph. Most results are of the type: if the network has a certain mesoscale structure, then also the dynamics have some structure [3, 32, 5]. In this work, we approach clustering from the other direction: we presume structure *in the dynamics* and aim to find all contact networks that are compatible with the structured dynamics. More specifically, we are interested in reducing the NIMFA dynamics (3) to

only a few differential equations. Hence, our results provide a framework to tame the complexity of epidemics on large contact networks.

The central analysis tool in our analysis is the *proper orthogonal decomposition* (POD) [6] of the $N \times 1$ viral state vector $v(t)$, which is given by

$$v(t) = \sum_{l=1}^{m} c_l(t) y_l \tag{5}$$

for some $m \leq N$. Here, the $N \times 1$ *agitation mode* vectors $y_1, ..., y_m$ are orthonormal[1], and the scalar functions $c_l(t) = y_l^T v(t)$ are obtained by projecting the viral state $v(t)$ onto the vector y_l. Since any $N \times 1$ vector $v(t)$ can be written as the linear combination of N orthonormal vectors, the POD (5) is exact for *any* network if $m = N$. However, we are particularly interested in networks, for which the number of agitation modes m is (much) smaller than the number of nodes N. If (5) holds true, then the viral state vector $v(t)$ is element of the m dimensional subspace

$$\mathcal{V} = \text{span}\{y_1, ..., y_m\} \tag{6}$$

at any time t, where the span (the set of all linear combinations) of the vectors $y_1, ..., y_m$ is denoted by

$$\text{span}\left\{y_1, ..., y_m\right\} = \left\{ \sum_{l=1}^{m} c_l y_l \Big| c_l \in \mathbb{R} \right\}.$$

With the POD (5), the viral state $v(t)$ can be described with less than N differential equations: denote the right side of the NIMFA (2) by $f_{\text{NIMFA}}\left(v(t)\right) \in \mathbb{R}^N$. Then, NIMFA (2) reads more compactly

$$\frac{dv(t)}{dt} = f_{\text{NIMFA}}\left(v(t)\right). \tag{7}$$

With the POD (5), we obtain that

$$\sum_{l=1}^{m} \frac{dc_l(t)}{dt} y_l = f_{\text{NIMFA}}\left(\sum_{l=1}^{m} c_l(t) y_l \right). \tag{8}$$

Since the vectors $y_1, ..., y_m$ are orthonormal, we can project (8) onto the agitation modes y_l to obtain the differential equations

$$\frac{dc_l(t)}{dt} = y_l^T f_{\text{NIMFA}}\left(\sum_{l=1}^{m} c_l(t) y_l \right), \quad l = 1, ..., m. \tag{9}$$

Hence, the POD (5) reduces the number of differential equations from the number of nodes N to the number of agitation modes m. We emphasise that the POD (5) is a hybrid of linear and nonlinear analysis: The viral state $v(t)$ equals a linear combination of the agitation modes y_l, which are weighted by possibly nonlinear functions $c_l(t)$. In [41], we have shown that the POD (5) is an accurate approximation for a diverse class of dynamics on networks. In this work, we study under which conditions the POD (5) is *exact* for the NIMFA epidemic model (2).

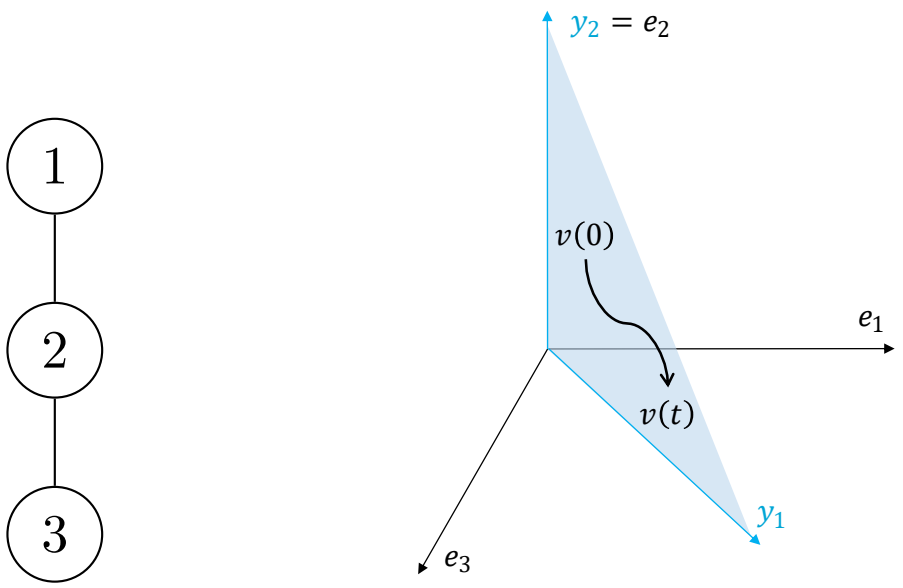

(a) Path graph.

(b) Viral state space.

Figure 1: **Proper orthogonal decomposition for a path graph. (a)**: A path graph with $N = 3$ nodes. The top, middle and bottom nodes are labelled by 1, 2 and 3, respectively. **(b)**: The black curve depicts the trajectory of the viral state $v(t)$ in the Euclidean space $\mathbb{R}^3$. The shaded area illustrates the viral state set $\mathcal{V}$, which equals the span of the vectors y_1, y_2, given by (12). Provided that $v(0) \in \mathcal{V}$, the viral state $v(t)$ remains in the subspace $\mathcal{V}$ at every time t.

Example 1. *Consider homogeneous NIMFA (3) on the path graph in Figure 1a, for which the viral state vector $v(t)$ evolves as*

$$\begin{aligned}
\frac{dv_1(t)}{dt} &= -\delta v_1(t) + \beta\,(1 - v_1(t))\,v_2(t), \\
\frac{dv_2(t)}{dt} &= -\delta v_2(t) + \beta\,(1 - v_2(t))\,(v_1(t) + v_3(t))\,, \\
\frac{dv_3(t)}{dt} &= -\delta v_3(t) + \beta\,(1 - v_3(t))\,v_2(t).
\end{aligned} \tag{10}$$

Suppose that the initial viral states of node 1 and 3 are equal, $v_1(0) = v_3(0)$. Then, it holds that $v_1(t) = v_3(t)$ at all times t due to the symmetry of the path graph. Hence, the viral state vector $v(t) = (v_1(t), v_2(t), v_3(t))^T$ satisfies

$$v(t) = c_1(t)y_1 + c_2(t)y_2, \tag{11}$$

where the orthonormal vectors y_1, y_2 are given by

$$y_1 = \frac{1}{\sqrt{2}}\begin{pmatrix}1\\0\\1\end{pmatrix}, \quad y_2 = \begin{pmatrix}0\\1\\0\end{pmatrix}. \tag{12}$$

[1] A set of vectors $y_1, ..., y_m$ is orthonormal if $y_l^T y_k = 0$ for $l \neq k$ and $y_l^T y_k = 1$ for $l = k$.

As illustrated by Figure 1b, the viral state $v(t)$ remains in the $m = 2$ dimensional subspace $\mathcal{V} = \text{span}\{y_1, y_2\}$ at all times t, provided that $v(0) \in \mathcal{V}$. On the subspace $\mathcal{V}$, (9) yields that the $N = 3$ differential equations (10) reduce to $m = 2$ equations

$$\frac{dc_1(t)}{dt} = -\delta c_1(t) + \sqrt{2}\beta \left(1 - \frac{1}{\sqrt{2}} c_1(t)\right) c_2(t),$$
$$\frac{dc_2(t)}{dt} = -\delta c_2(t) + 2\sqrt{2}\beta \left(1 - c_2(t)\right) c_1(t),$$

from which the viral state $v(t)$ is obtained with (11).

Two conditions must hold for the set $\mathcal{V}$ to reduce NIMFA to m differential equations. First, the set $\mathcal{V}$ must be an m dimensional subspace, spanned by the basis vectors $y_1, ..., y_m$. Second, if the initial viral state $v(0)$ is element of the set $\mathcal{V}$, then the viral state $v(t)$ must remain in the set $\mathcal{V}$ at every time $t > 0$. Hence, the set $\mathcal{V}$ must be an *invariant set* of NIMFA. Thus, we consider the geometric problem:

Problem 1 (Clustering in NIMFA)**.** *For a given number of nodes N and a given number $m \leq N$ of agitation modes, find* all *$N \times N$ infection rate matrices B and the corresponding $N \times 1$ agitation modes $y_1, ..., y_m$, such that $\mathcal{V} = \text{span}\{y_1, ..., y_m\}$ is an invariant set of NIMFA (2).*

In contrast to Example 1, for which the agitation modes y_1, y_2 follow rather straightforwardly, Problem 1 considers the interdependency of arbitrary graphs and invariant sets $\mathcal{V}$ in full generality.

If $m << N$, then we expect that the invariant set $\mathcal{V}$, and its basis vectors y_l, reflect a macroscopic structure, or a clustering, of the contact graph. For instance, the agitation mode y_1 in Example 1 indicates that the viral states $v_1(t)$ and $v_3(t)$ evolve equally and nodes 1 and 3 can be assigned to the same cluster.

Furthermore, the invariant set $\mathcal{V}$ allows for sophisticated, low-complexity control methods for the viral state $v(t)$, see [31] for a survey of control methods. More specifically, consider that an affine control method is applied to NIMFA (7),

$$\frac{dv(t)}{dt} = f_{\text{NIMFA}}\left(v(t)\right) + \sum_{l=1}^{m} g_l(t) y_l. \tag{13}$$

Here, the scalar function $g_l(t)$ is the control of the l-th agitation mode y_l. If the subspace $\mathcal{V} = \text{span}\{y_1, ..., y_m\}$ is an invariant set of NIMFA (2), then $\mathcal{V}$ is also an invariant set of (13). Hence, on the subspace $\mathcal{V}$, the viral state $v(t)$ can be controlled with only m distinct control inputs $g_1(t), ..., g_m(t)$. If the agitation mode y_l corresponds to a group of nodes, such as in Example 1, then the control $g_l(t)$ is applied to all nodes of that group. For instance, $g_l(t)$ could be the viral state control of individuals of a certain age group and location.

2 Related work

Clustering in NIMFA is closely related to *equitable partitions* [47, 56, 46]. We denote a general partition of the node set $\mathcal{N} = \{1, ..., N\}$ by[2] $\pi = \{\mathcal{N}_1, ..., \mathcal{N}_r\}$. Here, the *cells* $\mathcal{N}_1, ..., \mathcal{N}_r$ are disjoint subsets of

[2]Slightly deviating from common notation, we also refer to π as an (equitable) partition *of the infection rate matrix* B.

the node set $\mathcal{N}$, such that $\mathcal{N} = \mathcal{N}_1 \cup ... \cup \mathcal{N}_r$. We adapt the definition of *equitable* partitions in [29, 33] as:

Definition 2 (Equitable partition)**.** *Consider a symmetric $N \times N$ infection rate matrix B and a partition $\pi = \{\mathcal{N}_1, ..., \mathcal{N}_r\}$ of the node set $\mathcal{N} = \{1, ..., N\}$. The partition π is* equitable *if, for all cells $l, p = 1, ..., r$, the infection rates β_{ik} satisfy*

$$\sum_{k \in \mathcal{N}_l} \beta_{ik} = \sum_{k \in \mathcal{N}_l} \beta_{jk} \quad \forall i, j \in \mathcal{N}_p.$$

For an equitable partition π, we define the degree from cell $\mathcal{N}_l$ to cell $\mathcal{N}_p$ as

$$d_{pl} = \sum_{k \in \mathcal{N}_l} \beta_{ik} \tag{14}$$

for some node $i \in \mathcal{N}_p$. Definition 2 states that, for an equitable partition π, the sum of the infection rates (14) is the same for all nodes $i \in \mathcal{N}_p$. We denote the $r \times r$ *quotient matrix* by B^π, whose elements are defined as $(B^\pi)_{pl} = d_{pl}$. Furthermore, we define the $r \times 1$ all-one vector $u_r = (1, ..., 1)^T$.

As shown by Bonaccorsi *et al.* [5] and Ottaviano *et al.* [33], NIMFA (2) can be reduced to r differential equations, provided that the infection rate matrix B has an equitable partition π with r cells. For our work, we summarise the results in [5, 33] as:

Theorem 1 ([5, 33])**.** *Consider NIMFA (2) on an $N \times N$ infection rate matrix B with an equitable partition $\pi = \{\mathcal{N}_1, ..., \mathcal{N}_r\}$. Assume that $\delta_i = \delta_j$ and $v_i(0) = v_j(0)$ for all nodes i, j in the same cell $\mathcal{N}_l$. Then, it holds that $v_i(t) = v_j(t)$ at every time $t > 0$ for all nodes $i, j \in \mathcal{N}_l$ and all $l = 1, ..., r$. Furthermore, define the $r \times 1$* reduced-size *viral state vector $v^\pi(t) = (v_{i_1}(t), ..., v_{i_r}(t))^T$ and the $r \times r$* reduced-size *curing rate matrix*

$$S^\pi = \operatorname{diag}(\delta_{i_1}, ..., \delta_{i_r}), \tag{15}$$

where i_l denotes an arbitrary node in the cell $\mathcal{N}_l$. Then, the reduced-size viral state vector $v^\pi(t)$ evolves as

$$\frac{dv^\pi(t)}{dt} = -S^\pi v^\pi(t) + \operatorname{diag}(u_r - v^\pi(t)) B^\pi v^\pi(t). \tag{16}$$

Remarkably, on both microscopic (2) and macroscopic (16) resolutions, the viral dynamics follow the same class of governing equation. For the Markovian Susceptible-Infectious-Susceptible (SIS) process, Simon et *al.* [48] proposed a lumping approach to reduce the complexity, which is an approximation and merges states of the SIS Markov chain, also see the work of Ward *et al.* [61]. In [11], a generalised mean-field framework for Markovian SIS epidemics has been proposed, which includes NIMFA as a special case. Beyond epidemics, analogous results to Theorem 1 have been proved for a diverse set of dynamics[3] on networks with equitable partitions [13, 32, 37, 45, 12]. As a direct consequence of Theorem 1, equitable partitions are related to the proper orthogonal decomposition (5):

[3]Specifically, we believe that Theorem 1 can be generalised to the dynamics $\frac{dv_i(t)}{dt} = -\delta_i v_i(t) + \sum_{j=1}^N \beta_{ij} g(v_i(t), v_j(t))$, where the arbitrary function $g(v_i(t), v_j(t))$ describes the "coupling" [51, 4, 26, 41] between node i and j.

Corollary 1. *Consider NIMFA (2) on an $N \times N$ infection rate matrix B with an equitable partition $\pi = \{\mathcal{N}_1, ..., \mathcal{N}_r\}$. Assume that $\delta_i = \delta_j$ and $v_i(0) = v_j(0)$ for all nodes i, j in the same cell $\mathcal{N}_l$. Then, the subspace $\mathcal{V} = \text{span}\{y_1, ..., y_m\}$ with $m = r$ is an invariant set, where the $N \times 1$ agitation modes y_l are given by*

$$(y_l)_i = \begin{cases} \frac{1}{\sqrt{|\mathcal{N}_l|}} & \text{if} \quad i \in \mathcal{N}_l, \\ 0 & \text{if} \quad i \notin \mathcal{N}_l, \end{cases}$$

and the scalar functions equal $c_l(t) = \sqrt{|\mathcal{N}_l|} v_l^{\pi}(t)$.

In other words, Corollary 1 states that every equitable partition π yields an invariant set $\mathcal{V}$, whose dimension equals the number of cells r in the partition π. Example 2 illustrates Theorem 1 and Corollary 1:

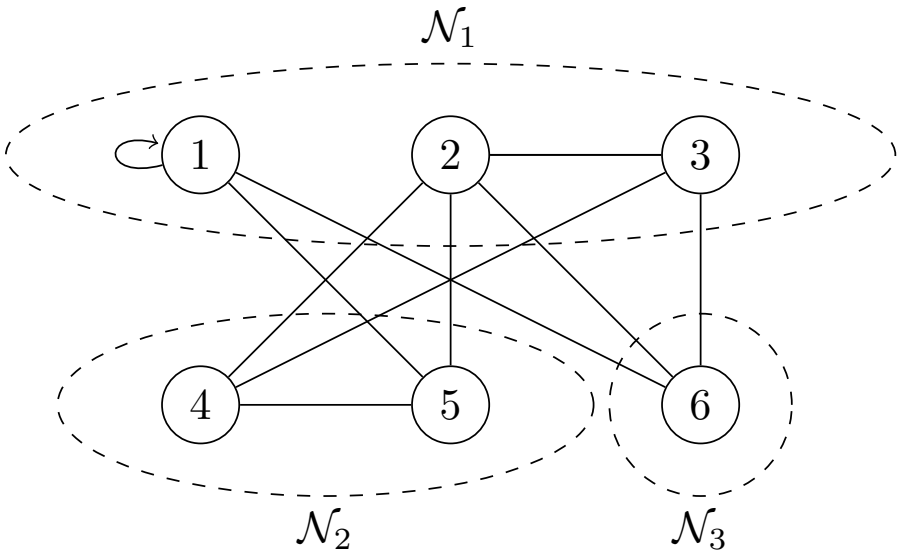

Figure 2: **Graph with a partition of the node set.** A graph with $N = 6$ nodes and the partition $\pi = \{\mathcal{N}_1, \mathcal{N}_2, \mathcal{N}_3\}$, whose cells are given by $\mathcal{N}_1 = \{1, 2, 3\}$, $\mathcal{N}_2 = \{4, 5\}$ and $\mathcal{N}_3 = \{6\}$. For unit link weights, i.e., $\beta_{ij} = 1$ for all nodes i, j, the partition π is *not* equitable. If the link weights β_{ij} satisfy (17), as in Example 2, then the partition π is equitable.

Example 2. *Consider NIMFA on a graph with $N = 6$ nodes, whose curing rate matrix equals $S = \text{diag}\left(\tilde{\delta}_1, \tilde{\delta}_1, \tilde{\delta}_1, \tilde{\delta}_2, \tilde{\delta}_2, \tilde{\delta}_3\right)$ for some curing rates $\tilde{\delta}_1, \tilde{\delta}_2, \tilde{\delta}_3$. Furthermore, suppose that the infection rate matrix B is symmetric and given by the graph in Figure 2 as*

$$B = \left(\begin{array}{ccc:ccc} \beta_{11} & 0 & 0 & 0 & \beta_{15} & \beta_{16} \\ 0 & 0 & \beta_{23} & \beta_{24} & \beta_{25} & \beta_{26} \\ 0 & \beta_{23} & 0 & \beta_{34} & 0 & \beta_{36} \\ \hdashline 0 & \beta_{24} & \beta_{43} & 0 & \beta_{45} & 0 \\ \beta_{15} & \beta_{25} & 0 & \beta_{45} & 0 & 0 \\ \hdashline \beta_{16} & \beta_{26} & \beta_{36} & 0 & 0 & 0 \end{array}\right).$$

Suppose that, for some degrees $d_{pl} > 0$, the infection rates β_{ij} satisfy: $\beta_{11} = \beta_{23} = d_{11}$; $\beta_{15} = \beta_{34} = d_{12}$ and $\beta_{24} = \beta_{25} = d_{12}/2$; $\beta_{16} = \beta_{26} = \beta_{36} = d_{13}$; and $\beta_{45} = d_{22}$. Then, the infection rate matrix B becomes

$$B = \left(\begin{array}{ccc:cc:c} d_{11} & 0 & 0 & 0 & d_{12} & d_{13} \\ 0 & 0 & d_{11} & d_{12}/2 & d_{12}/2 & d_{13} \\ 0 & d_{11} & 0 & d_{12} & 0 & d_{13} \\ \hdashline 0 & d_{12}/2 & d_{12} & 0 & d_{22} & 0 \\ d_{12} & d_{12}/2 & 0 & d_{22} & 0 & 0 \\ \hdashline d_{13} & d_{13} & d_{13} & 0 & 0 & 0 \end{array}\right). \tag{17}$$

Thus, the matrix B has the equitable partition $\pi = \{\mathcal{N}_1, \mathcal{N}_2, \mathcal{N}_3\}$ with the cells $\mathcal{N}_1 = \{1, 2, 3\}$, $\mathcal{N}_2 = \{4, 5\}$ and $\mathcal{N}_3 = \{6\}$. The quotient matrix equals

$$B^\pi = \begin{pmatrix} d_{11} & d_{12} & d_{13} \\ d_{12} & d_{22} & 0 \\ d_{13} & 0 & 0 \end{pmatrix}.$$

For the partition π, the reduced-size viral state can be chosen[4] as $v^\pi(t) = (v_1(t), v_4(t), v_6(t))^T$. Theorem 1 states that the vector $v^\pi(t) = (v_1(t), v_4(t), v_6(t))^T$ evolves as

$$\frac{dv^\pi(t)}{dt} = -S^\pi v^\pi(t) + \operatorname{diag}\left(u_3 - v^\pi(t)\right) B^\pi v^\pi(t),$$

with the 3×3 reduced-size curing rate matrix $S^\pi = \operatorname{diag}\left(\tilde{\delta}_1, \tilde{\delta}_2, \tilde{\delta}_3\right)$. Furthermore, Corollary 1 states that the viral state $v(t)$ has the proper orthogonal decomposition

$$v(t) = \sqrt{3} v_1^\pi(t) y_1 + \sqrt{2} v_2^\pi(t) y_2 + v_3^\pi(t) y_3$$

with the agitation modes

$$\begin{aligned} y_1 &= \frac{1}{\sqrt{3}} \begin{pmatrix} 1 & 1 & 1 & 0 & 0 & 0 \end{pmatrix}^T, \\ y_2 &= \frac{1}{\sqrt{2}} \begin{pmatrix} 0 & 0 & 0 & 1 & 1 & 0 \end{pmatrix}^T, \\ y_3 &= \begin{pmatrix} 0 & 0 & 0 & 0 & 0 & 1 \end{pmatrix}^T. \end{aligned}$$

3 Exact clustering

Theorem 1 and Corollary 1 only give an incomplete answer to Problem 1: if the infection rate matrix B has an equitable partition π, then there exists an invariant set $\mathcal{V}$. But are there invariant sets $\mathcal{V}$, even if the matrix B does not have an equitable partition π?

We denote the *orthogonal complement* of the viral state set $\mathcal{V}$ by

$$\mathcal{V}^\perp = \left\{ w \in \mathbb{R}^N | w^T v = 0, \quad \forall v \in \mathcal{V} \right\}.$$

[4] But, for instance, $v^\pi(t) = (v_2(t), v_5(t), v_6(t))^T$ is possible as well.

The dimension of the set $\mathcal{V}$ equals m. Thus, the dimension of the orthogonal complement $\mathcal{V}^\perp$ equals $N-m$. Since the orthogonal complement $\mathcal{V}^\perp$ is a subspace, there is a set of $N-m$ orthonormal basis vectors $y_{m+1}, ..., y_N$ such that

$$\mathcal{V}^\perp = \text{span}\{y_{m+1}, ..., y_N\}. \tag{18}$$

The *direct sum* of two subspaces $\mathcal{S}_1, \mathcal{S}_2 \subseteq \mathbb{R}^N$ is defined as the subspace

$$\mathcal{S}_1 \oplus \mathcal{S}_2 = \{s_1 + s_2 | s_1 \in \mathcal{S}_1, s_2 \in \mathcal{S}_2\}. \tag{19}$$

Thus, the Euclidean space is the direct sum $\mathbb{R}^N = \mathcal{V} \oplus \mathcal{V}^\perp$ of the two subspaces $\mathcal{V}, \mathcal{V}^\perp$.

We rely on four assumptions to solve Problem 1.

Assumption 1. *For every viral state $v \in \mathcal{V}$, we require that* $\text{diag}(\delta_1, ..., \delta_N)\, v \in \mathcal{V}$.

Suppose that the curing rates are homogeneous, i.e., $\delta_i = \delta$ for all nodes i. Then, Assumption 1 is satisfied, since $\text{diag}(\delta_1, ..., \delta_N)\, v = \delta v \in \mathcal{V}$ for every viral state $v \in \mathcal{V}$. More generally, Assumption 1 states that the viral state set $\mathcal{V}$ is an invariant subspace of the curing rate matrix $\text{diag}(\delta_1, ..., \delta_N)$. Intuitively speaking, the curing rates $\delta_1, ..., \delta_N$ are "set in accordance to" the clustering given by the viral state set $\mathcal{V}$, such as in Example 2.

Assumption 2. *There is a viral state $v \in \mathcal{V}$ whose entries satisfy $v_i > 0$ for every node $i = 1, ..., N$.*

If $R_0 > 1$ and the matrix B is irreducible, then [25] there is a unique steady-state v_∞ with positive components $v_{\infty,i} > 0$. Since every viral state v converges to the steady state v_∞, the steady state v_∞ is element of the invariant set $\mathcal{V}$. Hence, Assumption 2 is always satisfied if $R_0 > 1$, provided the matrix B is irreducible.

Assumption 3. *The curing rates are positive and the infection rates are non-negative, i.e., $\delta_i > 0$ and $\beta_{ij} \geq 0$ for all nodes i, j.*

Assumption 3 is rather technical, since only non-negative curing rates and infection rates have a physical meaning.

Assumption 4. *The infection rate matrix B is symmetric and irreducible.*

Assumption 4 holds if and only if the infection rate matrix B corresponds to a connected undirected graph [59]. Under Assumption 4, the matrix B is diagonalisable [56] as

$$B = X \Lambda X^T. \tag{20}$$

Here, we denote the $N \times N$ diagonal matrix $\Lambda = \text{diag}(\lambda_1, ..., \lambda_N)$ whose diagonal entries are given by the real eigenvalues $\lambda_1 \geq \lambda_2 \geq ... \geq \lambda_N$, and the columns of the $N \times N$ matrix $X = (x_1, ..., x_N)$ are given by the corresponding eigenvectors x_i.

Lemma 1 states that the invariant set $\mathcal{V}$ and the orthogonal complement $\mathcal{V}^\perp$ are spanned by eigenvectors of the infection rate matrix B:

Lemma 1. *Suppose that Assumptions 1 and 4 hold, and consider an invariant set* $\mathcal{V} = \text{span}\{y_1, ..., y_m\}$ *of NIMFA (2) and the orthogonal complement* $\mathcal{V}^\perp = \text{span}\{y_{m+1}, ..., y_N\}$*. Then, there is some permutation* ϕ*, i.e., a bijective mapping from the node set* $\{1, ..., N\}$ *to itself, such that* $\mathcal{V} = \text{span}\{x_{\phi(1)}, ..., x_{\phi(m)}\}$ *and* $\mathcal{V}^\perp = \text{span}\{x_{\phi(m+1)}, ..., x_{\phi(N)}\}$*, where* $x_{\phi(1)}, ..., x_{\phi(N)}$ *denotes an orthonormal set of eigenvectors of the infection rate matrix* B *to the eigenvalues* $\lambda_{\phi(1)}, ..., \lambda_{\phi(N)}$*.*

Proof. Appendix A □

We denote the span of the vectors $x_{\phi(l)}$ of the subspace $\mathcal{V}$ which correspond to a *non-zero* eigenvalue $\lambda_{\phi(l)} \neq 0$ as $\mathcal{V}_{\neq 0} = \text{span}\left\{x_{\phi(l)} \middle| l = 1, ..., m, \lambda_{\phi(l)} \neq 0\right\}$. Let the number of non-zero eigenvalues be denoted by m_1. Without loss of generality, we assume that, after the permutation ϕ, the *first* m_1 eigenvalues $\lambda_{\phi(1)}, ..., \lambda_{\phi(m_1)}$ are non-zero. Hence, the subspace $\mathcal{V}_{\neq 0}$ equals

$$\mathcal{V}_{\neq 0} = \text{span}\left\{x_{\phi(l)} \middle| l = 1, ..., m_1\right\}. \tag{21}$$

Analogously to (21), we define the span of the vectors $x_{\phi(l)}$ of the subspace $\mathcal{V}$ which correspond to a *zero* eigenvalue $\lambda_{\phi(l)} = 0$ as

$$\begin{aligned}\mathcal{V}_0 &= \text{span}\left\{x_{\phi(l)} \middle| l = 1, ..., m, \lambda_{\phi(l)} = 0\right\} \\ &= \text{span}\left\{x_{\phi(l)} \middle| l = m_1 + 1, ..., m\right\}.\end{aligned}$$

Thus, the subspace $\mathcal{V}$ is equal to the direct sum

$$\mathcal{V} = \mathcal{V}_{\neq 0} \oplus \mathcal{V}_0. \tag{22}$$

We emphasise that $\text{span}\{y_1, ..., y_m\} = \text{span}\left\{x_{\phi(1)}, ..., x_{\phi(m)}\right\}$ does not imply that $y_l = x_{\phi(k)}$ for some k, l. An immediate consequence of Lemma 1 is that the infection rate matrix B can be decomposed as:

Lemma 2. *Suppose that Assumptions 1 and 4 hold, and consider an invariant set* $\mathcal{V} = \text{span}\{y_1, ..., y_m\}$ *of NIMFA (2) and the orthogonal complement* $\mathcal{V}^\perp = \text{span}\{y_{m+1}, ..., y_N\}$*. Then, the infection rate matrix* B *is decomposable as* $B = B_{\mathcal{V}} + B_{\mathcal{V}^\perp}$*, where*

$$B_{\mathcal{V}} = \begin{pmatrix} y_1 & ... & y_m \end{pmatrix} \tilde{B}_{\mathcal{V}} \begin{pmatrix} y_1^T \\ \vdots \\ y_m^T \end{pmatrix} \quad \textit{and} \quad B_{\mathcal{V}^\perp} = \begin{pmatrix} y_{m+1} & ... & y_N \end{pmatrix} \tilde{B}_{\mathcal{V}^\perp} \begin{pmatrix} y_{m+1}^T \\ \vdots \\ y_N^T \end{pmatrix}$$

for some $m \times m$ *matrix* $\tilde{B}_{\mathcal{V}}$ *and* $(N-m) \times (N-m)$ *matrix* $\tilde{B}_{\mathcal{V}^\perp}$*.*

Proof. Appendix B. □

Lemma 2 shows that the sets $\mathcal{V}$ and $\mathcal{V}^\perp$ are invariant subspaces of the matrix B. In particular, the viral state dynamics on the invariant set $\mathcal{V}$ are the same for all infection rate matrices $B^{(1)}, B^{(2)}$ with the same submatrix $B^{(1)}_{\mathcal{V}} = B^{(2)}_{\mathcal{V}}$ but different submatrices $B^{(1)}_{\mathcal{V}^\perp} \neq B^{(2)}_{\mathcal{V}^\perp}$.

Example 3. *Suppose that Assumptions 1 and 4 hold. For some degrees d_{11}, d_{12}, d_{22} and some scalar ξ, consider the infection rate matrix*

$$B = \left(\begin{array}{cc:c} d_{11}+\xi & d_{11}-\xi & d_{12} \\ d_{11}-\xi & d_{11}+\xi & d_{12} \\ \hdashline d_{12} & d_{12} & d_{22} \end{array}\right).$$

Thus, the matrix B has the equitable partition $\pi = \{\mathcal{N}_1, \mathcal{N}_2\}$, where $\mathcal{N}_1 = \{1, 2\}$ and $\mathcal{N}_2 = \{3\}$, and the scalar ξ specifies the difference of the infection rate $\beta_{12} = d_{11} - \xi$ between nodes 1 and 2 and the self-infection rates $\beta_{11} = \beta_{22} = d_{11} + \xi$. The quotient matrix is given by

$$B^\pi = \begin{pmatrix} d_{11} & d_{12} \\ d_{12} & d_{22} \end{pmatrix}.$$

Corollary 1 states that the subspace $\mathcal{V} = \operatorname{span}\{y_1, y_2\}$ is an invariant set of NIMFA (2), where the agitation modes are equal to $y_1 = \frac{1}{\sqrt{2}}(1, 1, 0)^T$ and $y_2 = (0, 0, 1)^T$. The orthogonal complement follows as $\mathcal{V}^\perp = \operatorname{span}\{y_3\}$, where $y_3 = \frac{1}{\sqrt{2}}(1, -1, 0)^T$. Furthermore, Lemma 2 states that the infection rate matrix can be decomposed as $B = B_\mathcal{V} + B_{\mathcal{V}^\perp}$, where

$$B_\mathcal{V} = \begin{pmatrix} y_1 & y_2 \end{pmatrix} \begin{pmatrix} 2d_{11} & \sqrt{2}d_{12} \\ \sqrt{2}d_{12} & d_{22} \end{pmatrix} \begin{pmatrix} y_1^T \\ y_2^T \end{pmatrix} = \begin{pmatrix} d_{11} & d_{11} & d_{12} \\ d_{11} & d_{11} & d_{12} \\ d_{12} & d_{12} & d_{22} \end{pmatrix}$$

and

$$B_{\mathcal{V}^\perp} = 2\xi y_3 y_3^T = \begin{pmatrix} \xi & -\xi & 0 \\ -\xi & \xi & 0 \\ 0 & 0 & 0 \end{pmatrix}.$$

The eigenvectors $x_{\phi(1)}$, $x_{\phi(2)}$ are equal to a linear combination of the agitation modes y_1, y_2, and the third eigenvector equals $x_{\phi(3)} = y_3$.

Theorem 2 states our main result:

Theorem 2. *Suppose that Assumptions 1 to 4 hold. Then, any invariant set $\mathcal{V} = \operatorname{span}\{y_1, ..., y_m\}$ of NIMFA (2) is equal to the direct sum $\mathcal{V} = \mathcal{V}_{\neq 0} \oplus \mathcal{V}_0$ of two subspaces $\mathcal{V}_{\neq 0}$,$\mathcal{V}_0$. Here, the orthonormal basis vectors $y_1, ..., y_{m_1}$, where $m_1 \leq m$, of the subspace $\mathcal{V}_{\neq 0} = \operatorname{span}\{y_1, ..., y_{m_1}\}$ are given by*

$$(y_l)_i = \begin{cases} \frac{1}{\sqrt{|\mathcal{N}_l|}} & \text{if } i \in \mathcal{N}_l, \\ 0 & \text{if } i \notin \mathcal{N}_l, \end{cases} \tag{23}$$

for some equitable *partition $\pi = \{\mathcal{N}_1, ..., \mathcal{N}_{m_1}\}$ of the infection rate matrix B. If $m_1 = m$, then the subspace $\mathcal{V}_0$ is empty. Otherwise, if $m_1 < m$, then $\mathcal{V}_0 = \operatorname{span}\left\{x_{\phi(l)} \middle| l = m_1 + 1, ..., m\right\}$ for some eigenvectors $x_{\phi(l)}$ of the infection rate matrix B belonging to the eigenvalue 0.*

Proof. Appendix C. □

The Euclidean space $\mathbb{R}^N$ is always an invariant set of NIMFA. For $\mathcal{V} = \mathbb{R}^N$ and $\mathcal{V}_0 = \emptyset$, the equitable partition π in Theorem 2 becomes *trivial*, i.e., $\pi = \{\mathcal{N}_1, ..., \mathcal{N}_N\}$ with exactly one node in every cell $\mathcal{N}_l$. On the other hand, if there is an invariant set $\mathcal{V}$ of dimension $m < N$, then Theorem 2 implies that the matrix B is equitable with $m_1 \leq m$ cells.

If $\mathcal{V}_0 = \emptyset$, then Theorem 2 essentially reverts Corollary 1. Thus, every equitable partition π corresponds to an invariant set $\mathcal{V}_0$, and vice versa. *In other words, the macroscopic structure of equitable partitions π and the low-rank dynamics of invariant sets $\mathcal{V}$ are two sides of the same coin.* If $\mathcal{V}_0 = \emptyset$, then the dynamics on the invariant set $\mathcal{V} = \mathcal{V}_{\neq 0}$ are given by the reduced-size NIMFA system (16) with $m = m_1$ equations.

If $\mathcal{V}_0 \neq \emptyset$, then Theorem 2 is more general than the inversion of Corollary 1. Theorem 2 states that invariant set of NIMFA is equal to the direct sum $\mathcal{V} = \mathcal{V}_{\neq 0} \oplus \mathcal{V}_0$, where the subspace $\mathcal{V}_{\neq 0}$ corresponds to an equitable partition π of the infection rate matrix, and the subspace $\mathcal{V}_0$ is a subset of the kernel of the matrix B. If $\mathcal{V}_0 \neq \emptyset$, then the dynamics on the invariant set $\mathcal{V} = \mathcal{V}_{\neq 0} \oplus \mathcal{V}_0$ are described by the $m > m_1$ differential equations (9).

The curing rates δ_i satisfy Assumption 1 if there are some scalars $\tilde{\delta}_1, ..., \tilde{\delta}_{m_1}$ such that $\delta_i = \tilde{\delta}_l$ for all nodes i in cell $\mathcal{N}_l$, where $l = 1, ..., m_1$. However, Assumption 1 allows for more general curing rates. With Lemma 2 and Theorem 2, the infection rate matrix B can be constructed from specifying the agitation modes y_l, such that $\mathcal{V} = \text{span}\{y_1, ..., y_m\}$ is an invariant set of NIMFA (2):

Example 4. *Consider NIMFA (2) on a network of $N = 5$ nodes and the subspaces $\mathcal{V}_{\neq 0} = \text{span}\{y_1, y_2\}$, $\mathcal{V}_0 = \text{span}\{y_3\}$, where the agitation modes equal*

$$y_1 = \frac{1}{\sqrt{3}} \begin{pmatrix} 1 & 1 & 1 & 0 & 0 \end{pmatrix}^T,$$
$$y_2 = \frac{1}{\sqrt{2}} \begin{pmatrix} 0 & 0 & 0 & 1 & 1 \end{pmatrix}^T,$$
$$y_3 = \frac{1}{\sqrt{6}} \begin{pmatrix} 1 & -2 & 1 & 0 & 0 \end{pmatrix}^T.$$

Furthermore, let y_4, y_5 be two vectors, with $y_4^T y_5 = 0$ and $y_4^T y_4 = y_5^T y_5 = 1$, that are orthogonal to the agitation modes y_1, y_2, y_3. With Lemma 2, define the infection rate matrix as

$$B = \begin{pmatrix} y_1 & y_2 \end{pmatrix} \tilde{B}_{\mathcal{V}_{\neq 0}} \begin{pmatrix} y_1^T \\ y_2^T \end{pmatrix} + \begin{pmatrix} y_4 & y_5 \end{pmatrix} \tilde{B}_{\mathcal{V}^\perp} \begin{pmatrix} y_4^T \\ y_5^T \end{pmatrix},$$

where the symmetric 2×2 matrices $\tilde{B}_{\mathcal{V}_{\neq 0}}$, $\tilde{B}_{\mathcal{V}^\perp}$ are chosen such that the matrix B is irreducible and contains only non-negative elements. Furthermore, consider the curing rate matrix $S = \text{diag}(\tilde{\delta}_1, \tilde{\delta}_2, \tilde{\delta}_1, \tilde{\delta}_3, \tilde{\delta}_3)$ for some curing rates $\tilde{\delta}_1, \tilde{\delta}_2, \tilde{\delta}_3 > 0$. Then, Assumptions 1 to 4 are satisfied, and Theorem 2 states that the subspace $\mathcal{V} = \mathcal{V}_{\neq 0} \oplus \mathcal{V}_0$ is an invariant set of NIMFA (2). (An alternative choice for the curing rate matrix is $S = \text{diag}(\tilde{\delta}_1, \tilde{\delta}_1, \tilde{\delta}_1, \tilde{\delta}_2, \tilde{\delta}_2)$, which also satisfies Assumption 1.)

In [42], we derived the solution of the NIMFA model (2) around the epidemic threshold $R_0 = 1$. More precisely, under mild assumptions, we derived the approximation $v_{\text{apx}}(t) = c(t)v_\infty$ with an explicit, closed-form expression for the scalar function $c(t)$. If the initial viral state satisfies $\|v(0)\|_2 \leq \tilde{\sigma}(R_0 - 1)^2$ for some constant $\tilde{\sigma}$ as $R_0 \downarrow 1$, then it holds that $\|v(t) - v_{\text{apx}}(t)\|_2 \leq \sigma(R_0 - 1)^2$ at every time t for some constant σ as $R_0 \downarrow 1$. Hence, the viral state $v(t)$ converges to the approximation $v_{\text{apx}}(t)$

uniformly in time t. Remarkably, since $v_{\text{apx}} = c(t)v_\infty$, the viral state $v(t)$ lies in the one-dimensional subspace $\mathcal{V} = \text{span}\{v_\infty\}$ when $R_0 \downarrow 1$, for an arbitrarily large and heterogeneous contact network. Figure 3 illustrates the uniform convergence result in [42, Theorem 3].

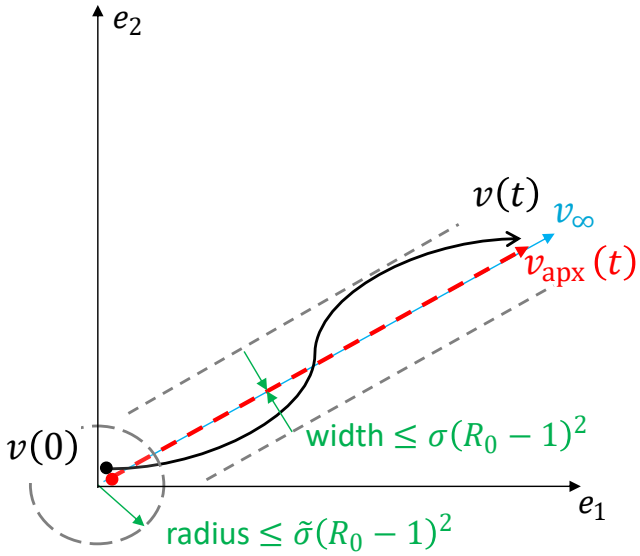

Figure 3: **Viral dynamics around the epidemic threshold $R_0 = 1$.** An illustration of the uniform convergence result in [42, Theorem 3] for a network with $N = 2$ nodes. The black curve shows the trajectory of the 2×1 viral state vector $v(t)$ as time t evolves. The blue line shows the steady state v_∞. The red curve depicts the trajectory closed-form approximation $v_{\text{apx}}(t) = c(t)v_\infty$, which is in the subspace $\text{span}\{v_\infty\}$ at every time t. If the initial viral state $v(0)$ is positive and in the disk of radius $\tilde{\sigma}\,(R_0 - 1)^2$ for some constant $\tilde{\sigma}$, then the approximation error $\|v(t) - v_{\text{apx}}(t)\|_2$ is bounded by $\sigma\,(R_0 - 1)^2$ for some constant σ at every time t as $R_0 \downarrow 1$.

As illustrated by Figure 3, the viral state $v(t)$ converges to the one-dimensional dynamics $v_{\text{apx}}(t)$ as $R_0 \downarrow 1$. *Are there networks for which the approximation $v_{\text{apx}}(t)$ is exact, for any basic reproduction number $R_0 > 1$?* The infection rate matrix B is *regular* if

$$\sum_{k=1}^{N} \beta_{ik} = \sum_{k=1}^{N} \beta_{jk} \tag{24}$$

for all nodes i, j. From Theorem 2, we obtain:

Corollary 2. *Suppose that Assumptions 1 to 4 hold and consider that $R_0 > 1$. Then, there is an $m = 1$ dimensional invariant set $\mathcal{V} = \text{span}\{y_1\}$ of NIMFA (2) if and only if $\mathcal{V}_0 = \emptyset$, the agitation mode equals either $y_1 = v_\infty/\|v_\infty\|_2$ or $y_1 = -v_\infty/\|v_\infty\|_2$ and the infection rate matrix B is regular. Furthermore, the approximation $v_{\text{apx}}(t) = c(t)v_\infty$ is exact if and only if the matrix B is regular and $v(0) = c(0)v_\infty$ for some scalar $c(0)$.*

Proof. Appendix D □

3.1 Decomposition of the viral dynamics

Suppose the infection rate matrix B has an equitable partition π and the infection rates β_{ij} are the same between all nodes i, j in any two cells[5]. Then, we can decompose the dynamics of the viral state $v(t)$ as:

Theorem 3. *Consider NIMFA (2) on a symmetric $N \times N$ infection rate matrix B with an equitable partition $\pi = \{\mathcal{N}_1, ..., \mathcal{N}_r\}$. Furthermore, suppose that the curing rates δ_i are the same for all nodes i in any cell $\mathcal{N}_l$, and that the infection rates β_{ij} are the same for all nodes i in any cell $\mathcal{N}_l$ and all nodes j in any cell $\mathcal{N}_p$. Denote the subspace $\mathcal{V}_{\neq 0} = \text{span}\{y_1, ..., y_r\}$, with the basis vectors y_l defined in (23), and denote the kernel of the matrix B by $\ker(B) = \text{span}\{y_{r+1}, ..., y_N\}$. At every time $t \geq 0$, consider the viral state decomposition*

$$v(t) = \tilde{v}(t) + v_{\ker}(t),$$

where the projection of the viral state $v(t)$ on the subspace $\mathcal{V}_{\neq 0}$ equals

$$\tilde{v}(t) = \sum_{l=1}^{r} \left(y_l^T v(t)\right) y_l,$$

and the projection of the viral state $v(t)$ on the kernel $\ker(B)$ equals

$$v_{\ker}(t) = \sum_{l=r+1}^{N} \left(y_l^T v(t)\right) y_l.$$

Furthermore, denote the $r \times 1$ reduced-size projection $\tilde{v}^\pi(t) = \left(\tilde{v}^\pi_{i_1}(t), ..., \tilde{v}^\pi_{i_r}(t)\right)^T$, where i_l denotes an arbitrary node in cell $\mathcal{N}_l$. Then, the reduced-size projection $\tilde{v}^\pi(t)$ evolves, independently of the projection $v_{\ker}(t)$, as

$$\frac{d\tilde{v}^\pi(t)}{dt} = -S^\pi \tilde{v}^\pi(t) + \text{diag}\left(u_r - \tilde{v}^\pi(t)\right) B^\pi \tilde{v}^\pi(t) \tag{25}$$

with the quotient matrix B^π and the matrix S^π given by (15), and the projection $v_{\ker}(t)$ obeys

$$\frac{dv_{\ker}(t)}{dt} = -\left(S + \text{diag}\left(B\tilde{v}(t)\right)\right) v_{\ker}(t). \tag{26}$$

Proof. Appendix E. □

In Theorem 3, the set $\mathcal{V}_0$ is equal to the kernel $\ker(B)$, which is equivalent to $\mathcal{V}^\perp = \emptyset$ and assuming the same infection rates β_{ij} between all nodes i, j in any two cells. In contrast to Theorem 1, we do not consider that the initial state satisfies $v_i(0) = v_j(0)$ for all nodes i, j in the same cell $\mathcal{N}_l$.

With the definition of the agitation mode y_l in (23), the viral state average in cell $\mathcal{N}_l$ follows from the projection of the viral state $v(t)$ on the vector y_l as

$$\frac{1}{|\mathcal{N}_l|} \sum_{i \in \mathcal{N}_l} v_i(t) = \frac{1}{\sqrt{|\mathcal{N}_l|}} y_l^T v(t)$$

[5]If the matrix B is decomposable as $B = B_{\mathcal{V}} + B_{\mathcal{V}^\perp}$ as in Lemma 2, then the infection rates β_{ij} are the same between all nodes i, j in any two cells if and only if $B_{\mathcal{V}^\perp} = 0$.

for every cell $l = 1, ..., r$. Furthermore, the subspace $\mathcal{V}_{\neq 0}$ is spanned by the vectors y_1, ..., y_r. Hence, the dynamics of the projection $\tilde{v}(t)$ on the subspace $\mathcal{V}_{\neq 0}$ describes the evolution of viral state averages of every cell $\mathcal{N}_l$, which is described by r differential equations (25) on the quotient graph B^π. Since the steady state $v_{\infty,i}$ of every node i in the same cell $\mathcal{N}_l$ is the same [5, 33], it holds that $v_\infty \in \mathcal{V}_{\neq 0}$, which implies that $v_{\ker}(t) \to 0$ as $t \to \infty$. Furthermore, from Theorem 1 it follows that, if $v_{\ker}(0) = 0$, then $v_{\ker}(t) = 0$ at every time t. Thus, the evolution of the projection $v_{\ker}(t)$ describes convergence of the viral states $v_i(t)$ to the respective cell-averages. *By (25), Theorem 3 implies that the viral state cell-averages evolve independently of the dynamics on the kernel* $\ker(B)$. Schaub *et al.* [45] obtained an analogous result for linear dynamics on networks.

If we can derive the closed-form expression for the projection $\tilde{v}(t)$ by solving (25), then the dynamics $v_{\ker}(t)$ follow by the linear time-*varying* system (26). Furthermore, the reduced-size steady state $v^\pi_\infty = \left(\tilde{v}^\pi_{\infty,i_1}, ..., \tilde{v}^\pi_{\infty,i_r}\right)^T$ is an equilibrium of (25). Thus, if $\tilde{v}(t) = v_\infty$, then the dynamics of the projection $v_{\ker}(t)$ obey the linear time-*invariant* (LTI) system

$$\frac{dv_{\ker}(t)}{dt} = -\left(S + \operatorname{diag}\left(Bv_\infty\right)\right) v_{\ker}(t).$$

Thus, the affine subspace $\left\{v_\infty + v_{\ker} \middle| v_{\ker} \in \ker(B)\right\}$ is an invariant set of NIMFA, on which the viral dynamics are linear.

Loosely speaking, Theorem 3 shows that a crucial challenge for solving NIMFA on graphs with equitable partitions is the dynamics of the projection $\tilde{v}(t)$, since solving the set of nonlinear equations (25) seems more difficult than solving the linear time-varying system (26) for a given $\tilde{v}(t)$. For a complete graph, the solution $\tilde{v}(t)$ to set of nonlinear equations (25) is one-dimensional and can be stated in closed form [53]. Thus, we obtain the solution of NIMFA on the complete graph, for *arbitrary* initial viral states $v(0)$, as:

Theorem 4. *Consider NIMFA (2) on the complete graph, whose infection rates equal $\beta_{ij} = \beta > 0$ for all nodes $i, j = 1, ..., N$. Suppose the curing rates satisfy $\delta_i = \delta$ for all nodes i. Then, for any initial viral state $v(0) \in [0, 1]^N$, the solution of NIMFA (2) equals*

$$v(t) = c_1(t)y_1 + c_2(t)v_{\ker}(0),$$

with the agitation mode $y_1 = u/\sqrt{N}$, and the $N \times 1$ vector $v_{\ker}(0)$ given by

$$v_{\ker}(0) = \left(I - y_1 y_1^T\right) v(0).$$

The functions $c_1(t)$ and $c_2(t)$ follow explicitly as:

1. *If $\delta \neq \beta N$, then the scalar function $c_1(t)$ equals*

$$c_1(t) = \frac{w}{2\beta\sqrt{N}}\left(1 + \tanh\left(\frac{w}{2}t + \Upsilon_1(0)\right)\right) \tag{27}$$

with the viral slope $w = \beta N - \delta$ *and the constant*

$$\Upsilon_1(0) = \operatorname{arctanh}\left(2\frac{\beta\sqrt{N}}{w}y_1^T v(0) - 1\right),$$

and the scalar function $c_2(t)$ *equals*

$$c_2(t) = \Upsilon_2(0)e^{-\Phi t}\,\mathrm{sech}\left(\frac{w}{2}t + \Upsilon_1(0)\right) \tag{28}$$

with the constants $\Phi = w/2 + \delta$ *and*

$$\Upsilon_2(0) = \frac{v_{\mathrm{ker}}^T(0)v(0)}{\|v_{\mathrm{ker}}(0)\|_2^2}\cosh\left(\Upsilon_1(0)\right). \tag{29}$$

2. *If* $\delta = \beta N$*, then the scalar function* $c_1(t)$ *equals*

$$c_1(t) = \sqrt{N}\left(\delta t + \frac{\sqrt{N}}{y_1^T v(0)}\right)^{-1} \tag{30}$$

and the scalar function $c_2(t)$ *obeys*

$$c_2(t) = \tilde{\Upsilon}_2(0)e^{-\delta t}\left(\delta t + \frac{\sqrt{N}}{y_1^T v(0)}\right)^{-\frac{\beta N}{\delta}},$$

where the constant $\tilde{\Upsilon}_2(0)$ *is given by*

$$\tilde{\Upsilon}_2(0) = \frac{v_{\mathrm{ker}}^T(0)v(0)}{\|v_{\mathrm{ker}}(0)\|_2^2}\left(\frac{\sqrt{N}}{y_1^T v(0)}\right)^{\frac{\beta N}{\delta}}.$$

Proof. Appendix F. □

Figure 4 illustrates the closed-form solution of NIMFA for complete graphs, as given by Theorem 4. In Figures 4a and 4b, even though the viral state average $\tilde{v}(t)$ is monotonically increasing, the viral state $v_1(t) = \tilde{v}_1(t) + v_{\mathrm{ker},1}(t)$ is decreasing until $t \approx 1$, which is due to the dynamics of the projection $v_{\mathrm{ker}}(t)$ on the kernel $\ker(B)$.

Theorem 4 implies that Conjecture 1 in [42] is wrong. More specifically, Theorem 4 shows that, at least for the complete graph and *general*[6] initial states $v(0)$, the viral state $v(t)$ does not converge to the approximation $v_{\mathrm{apx}}(t)$ with respect to the L_2-norm as $R_0 \downarrow 1$.

4 Approximate clustering

As shown by Theorem 2, equitable partitions and low-dimensional viral state dynamics in NIMFA are equivalent. Many networks possess some macroscopic structure, which may *resemble* an equitable partition, but which *is not precisely* an equitable partition. *Is it possible to reduce the number of NIMFA equations, if the network has an "almost" equitable partition?*

For two $N \times 1$ vectors x, y, $x \geq y$ denotes that $x_i \geq y_i$ for all entries $i = 1, ..., N$. Theorem 5 shows that NIMFA (2) on any network can be bounded by increasing or decreasing the spreading rates β_{ij},δ_i:

[6] In Figure 3, the initial viral state $v(0)$ was not general, since $\|v(0)\|_2 \leq \tilde{\sigma}(R_0 - 1)^2$ as $R_0 \downarrow 1$.

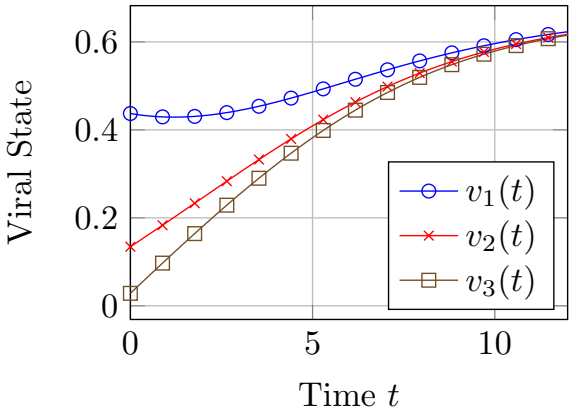

(a) Viral state $v(t)$ versus time t for a basic reproduction number of $R_0 = 1.3$.

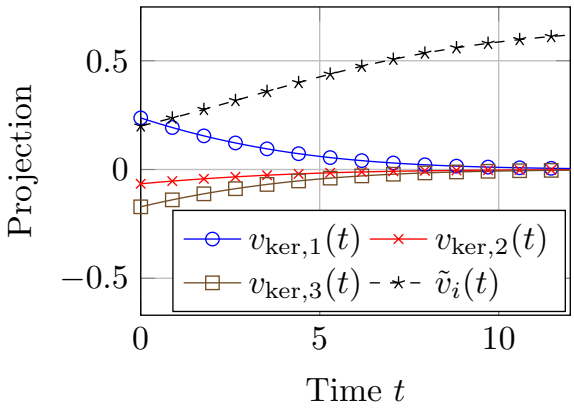

(b) The projections $v_{\text{ker},i}(t)$, $\tilde{v}_i(t)$ versus time t for a basic reproduction number of $R_0 = 1.3$.

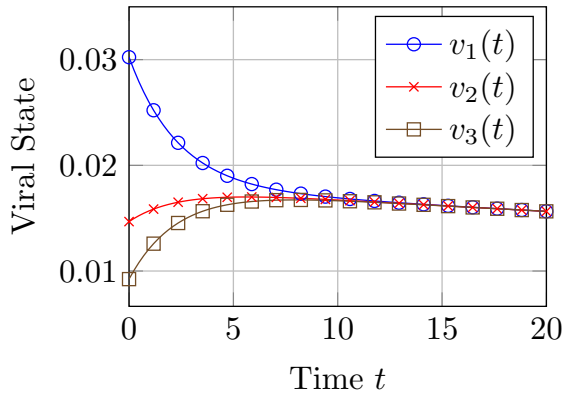

(c) Viral state $v(t)$ versus time t for a basic reproduction number of $R_0 = 1$.

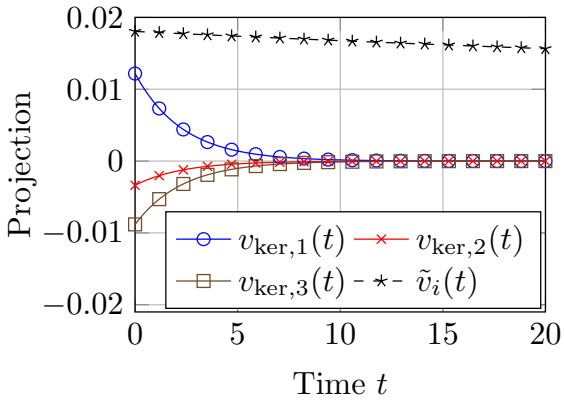

(d) The projections $v_{\text{ker},i}(t)$, $\tilde{v}_i(t)$ versus time t for a basic reproduction number of $R_0 = 1$.

Figure 4: **Closed-form solution of NIMFA on the complete graph.** The solution of NIMFA (1) for a complete graph with $N = 3$ nodes and homogeneous spreading rates. The first and second rows correspond to a basic reproduction number of $R_0 = 1.3$ and $R_0 = 1$, respectively. As stated by Theorem 3, the viral state satisfies $v(t) = \tilde{v}(t) + v_{\text{ker}}(t)$, where $\tilde{v}(t)$ and $v_{\text{ker}}(t)$ denote the projection of the viral state $v(t)$ on the subspace $\mathcal{V}_{\neq 0}$ and the kernel $\ker(B)$, respectively. **(a)**: The viral state $v_i(t)$ versus time t for every node i. **(b)**: The projections $\tilde{v}(t)$ and $v_{\text{ker}}(t)$, which follow from Theorem 4 as $\tilde{v}_i(t) = c_1(t)v_{\infty,i}$ and $v_{\text{ker},i}(t) = c_2(t)\,(y_2)_i$ for all nodes i, where the scalar functions $c_1(t)$ and $c_2(t)$ are given by the closed-form expressions (27) and (28), respectively. Since the steady state $v_{\infty,i}$ is the same for every node i in the complete graph, it holds that $\tilde{v}_i(t) = \tilde{v}_j(t)$ for all nodes i, j. **(c),(d)**: The same plots as in the first row, but with a basic reproduction number of $R_0 = 1$ instead of $R_0 = 1.3$.

Theorem 5. *Consider two NIMFA systems with respective positive curing rates δ_i and $\tilde{\delta}_i$, non-negative infection rates β_{ij} and $\tilde{\beta}_{ij}$, and viral states $v_i(t)$ and $\tilde{v}_i(t)$. Suppose that the initial viral state $v_i(0)$,$\tilde{v}_i(0)$ are in $[0, 1]$ for all nodes i and that the matrices B and $\tilde{B}$, with elements β_{ij} and $\tilde{\beta}_{ij}$, respectively, are irreducible. Then, if $\tilde{\delta}_i \leq \delta_i$ and $\tilde{\beta}_{ij} \geq \beta_{ij}$ for all nodes i, j, $\tilde{v}(0) \geq v(0)$ implies that $\tilde{v}(t) \geq v(t)$ at every time t.*

Proof. Appendix G. □

We emphasise that Theorem 5 does not assume symmetric infection rate matrices B, $\tilde{B}$. Building upon Theorem 5, we aim to bound the viral state $v(t)$ of any network at every time t by the viral state of networks with equitable partitions. In the following, we consider a partition $\pi = \{\mathcal{N}_1, ..., \mathcal{N}_r\}$ of the node set $\mathcal{N} = \{1, ..., N\}$ of an arbitrary network. We stress that π can be *any*, not necessarily equitable, partition. We define the minimum $d_{\min,pl}$ of the sum of infection rates from cell $\mathcal{N}_l$ to $\mathcal{N}_p$ as

$$d_{\min,pl} = \min_{i \in \mathcal{N}_p} \sum_{k \in \mathcal{N}_l} \beta_{ik} \tag{31}$$

and the maximum $d_{\max,pl}$ as

$$d_{\max,pl} = \max_{i \in \mathcal{N}_p} \sum_{k \in \mathcal{N}_l} \beta_{ik}. \tag{32}$$

Furthermore, we denote the $r \times r$ matrices $B_{\min}$ and $B_{\max}$, whose elements are given by $d_{\min,pl}$ and $d_{\max,pl}$, respectively. Analogously, we define the minimum $\delta_{\min,l}$ of the curing rates in cell $\mathcal{N}_l$ as

$$\delta_{\min,l} = \min_{i \in \mathcal{N}_l} \delta_i$$

and the maximum $\delta_{\max,l}$ as

$$\delta_{\max,l} = \max_{i \in \mathcal{N}_l} \delta_i. \tag{33}$$

We combine Theorem 1 and Theorem 5 to obtain:

Theorem 6. *Suppose that the Assumptions 3 and 4 hold. At every time t, consider the $r \times 1$ reduced-size lower bound $v_{\mathrm{lb},l}(t)$ and $r \times 1$ upper bound $v_{\mathrm{ub},l}(t)$, which evolve as*

$$\frac{dv_{\mathrm{lb}}(t)}{dt} = -\operatorname{diag}\left(\delta_{\max,1}, ..., \delta_{\max,r}\right) v_{\mathrm{lb}}(t) + \operatorname{diag}\left(u_r - v_{\mathrm{lb}}(t)\right) B_{\min} v_{\mathrm{lb}}(t) \tag{34}$$

and

$$\frac{dv_{\mathrm{ub}}(t)}{dt} = -\operatorname{diag}\left(\delta_{\min,1}, ..., \delta_{\min,r}\right) v_{\mathrm{ub}}(t) + \operatorname{diag}\left(u_r - v_{\mathrm{ub}}(t)\right) B_{\max} v_{\mathrm{ub}}(t).$$

Then, if the initial states satisfy $v_{\mathrm{lb},l}(0) \leq v_i(0) \leq v_{\mathrm{ub},l}(0)$ for all nodes i in any cell $\mathcal{N}_l$, the viral state $v_i(t)$ of all nodes i in any cell $\mathcal{N}_l$ is bounded by

$$v_{\mathrm{lb},l}(t) \leq v_i(t) \leq v_{\mathrm{ub},l}(t) \quad \forall t \geq 0. \tag{35}$$

Proof. Appendix H. □

Theorem 6 states that the $N \times 1$ viral state $v(t)$ on *any* network is bounded by the $r \times 1$ viral states $v_{\mathrm{lb}}(t)$, $v_{\mathrm{ub}}(t)$ on networks with equitable partitions and r cells. Reducing the N-dimensional viral state dynamics to r-dimensional dynamics comes at the cost of an *approximate* description by the bounds in (35). If the partition π is equitable, then it holds that $d_{\min,pl} = d_{\max,pl}$, and the bounds in Theorem 6 can be replaced by the exact statement in Theorem 1.

Similarly to the lower bound and upper bound of the degrees in (31) and (32), respectively, we define the *average* degree from cell $\mathcal{N}_l$ to $\mathcal{N}_p$ for any partition π as

$$\bar{d}_{pl} = \frac{1}{|\mathcal{N}_p|} \sum_{i \in \mathcal{N}_p} \sum_{k \in \mathcal{N}_l} \beta_{ik}.$$

Then, we define the $r \times r$ reduced-size infection rate matrix $\bar{B}$, which consists of the elements $\bar{d}_{pl}$. Furthermore, we define the average curing rate of any cell $\mathcal{N}_l$ as

$$\bar{\delta}_l = \frac{1}{|\mathcal{N}_l|} \sum_{i \in \mathcal{N}_l} \delta_i.$$

Then, we approximate the viral state by $v_i(t) \approx \bar{v}_l(t)$ for all nodes i in any cell $\mathcal{N}_l$. Here, the $r \times 1$ reduced-size viral state vector $\bar{v}(t)$ evolves as

$$\frac{d\bar{v}(t)}{dt} = -\operatorname{diag}\left(\bar{\delta}_1, ..., \bar{\delta}_r\right) \bar{v}(t) + \operatorname{diag}\left(u_r - \bar{v}(t)\right) \bar{B}\bar{v}(t), \tag{36}$$

and, for all cells $\mathcal{N}_l$, the initial state equals

$$\bar{v}_l(0) = \frac{1}{|\mathcal{N}_l|} \sum_{i \in \mathcal{N}_l} v_l(0).$$

If the matrix B has an equitable partition π and the rates δ_i, β_{ij} are the same between all nodes i, j in any two cells as in Theorem 3, then the approximation $\bar{v}(t)$ coincides with the projection $\tilde{v}(t)$ of the viral state $v(t)$ on the subspace $\mathcal{V}_{\neq 0}$.

To illustrate the accuracy of the bounds in Theorem 6 and the reduced-size viral state $\bar{v}(t)$ for networks without equitable partitions, we consider the *Stochastic Blockmodel* (SBM), originally introduced by Holland *et al.* [20]. We consider a network with $N = 1000$ nodes and a partition π with $r = 5$ cells $\mathcal{N}_1$, ..., $\mathcal{N}_5$. The cells are of size $|\mathcal{N}_1| = 400$, $|\mathcal{N}_2| = 250$, $|\mathcal{N}_3| = 200$, $|\mathcal{N}_4| = 100$ and $|\mathcal{N}_5| = 50$. With a probability of 0.7, there are no links between two cells $\mathcal{N}_p$, $\mathcal{N}_l$, i.e., $\beta_{ij} = \beta_{ji} = 0$ for all nodes $i \in \mathcal{N}_p$ and $j \in \mathcal{N}_l$. Otherwise, with a probability of 0.3, we denote the mean of the links between the cells $\mathcal{N}_p$, $\mathcal{N}_l$ by $\bar{\beta}_{pl} = \bar{\beta}_{lp}$, which is set to a uniform random number in $[0.1, 0.2]$. Then, the infection rate $\beta_{ij} = \beta_{ji}$ for all nodes $i \in \mathcal{N}_p$ and $j \in \mathcal{N}_l$ is set to a random number $[\bar{\beta}_{pl}, \bar{\beta}_{pl}(1 + \sigma_{\text{rel}})]$, where we vary the *relative variance* σ_{rel} for different scenarios in the numerical evaluation. If $\sigma_{\text{rel}} = 0$, then the partition π is equitable. The larger the variance σ_{rel}, the "less equitable" the partition π. For every node i, the curing rate δ_i is set to a uniform random number in $[1, 1 + \sigma_{\text{rel}}]$, and the initial viral state $v_i(0)$ is set to a uniform random number in $[0.01, 0.01(1 + \sigma_{\text{rel}})]$. Hence, if the variance $\sigma_{\text{rel}} = 0$, then it holds that $v_{\text{lb},l}(t) = v_{\text{lb},l}(t) = v_i(t)$ for every node i in any cell $\mathcal{N}_l$. Lastly, the curing rates are decreased to $\delta_i \leftarrow c\delta_i$, where the scalar c is chosen such that the basic reproduction number (4) equals $R_0 = 3$. To obtain the viral state $v(t)$, we discretise NIMFA (1) with a sufficiently small sampling time, see [34, 40, 27] for a detailed analysis of the resulting discrete-time NIMFA model.

Figure 5 illustrates the accuracy of the bounds $v_{\text{lb},l}(t)$, $v_{\text{ub},l}(t)$ in Theorem 6 and the approximation accuracy of $\bar{v}(t)$ in (36) for the largest cell $\mathcal{N}_1$ and the smallest cell $\mathcal{N}_5$. For both $\sigma_{\text{rel}} = 0.25$ and $\sigma_{\text{rel}} = 0.5$, the approximation $\bar{v}_l(t)$ is close to the exact average viral state in cell $\mathcal{N}_l$,

$$v_{\text{avg},l}(t) = \frac{1}{|\mathcal{N}_l|} \sum_{i \in \mathcal{N}_l} v_l(t).$$

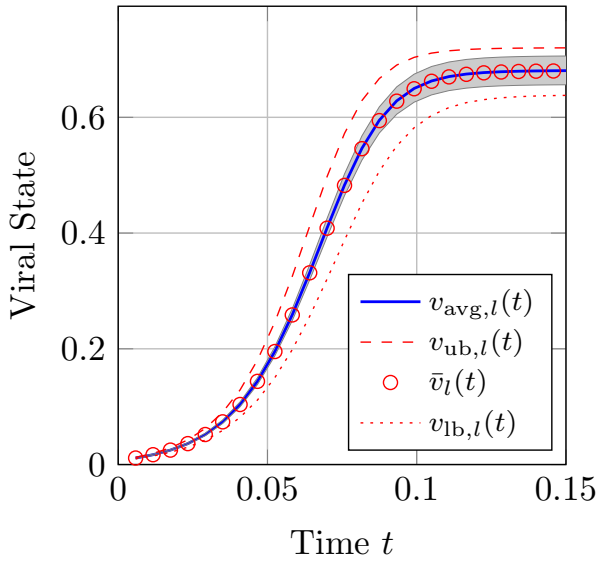

(a) Cell $\mathcal{N}_1$ and relative variance $\sigma_{\mathrm{rel}} = 0.25$.

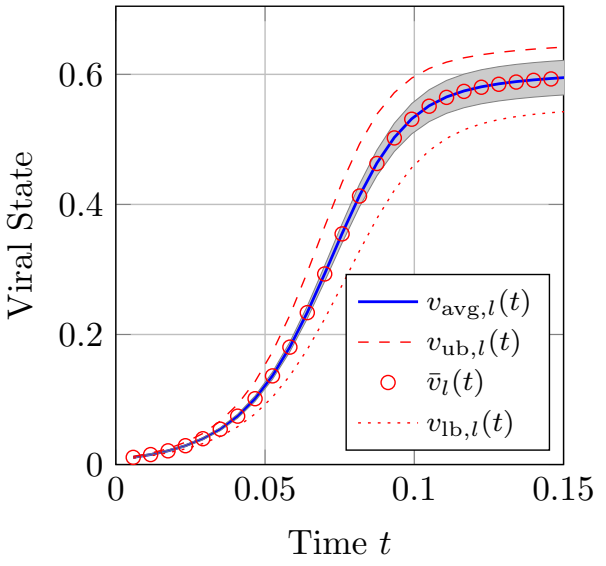

(b) Cell $\mathcal{N}_5$ and relative variance $\sigma_{\mathrm{rel}} = 0.25$.

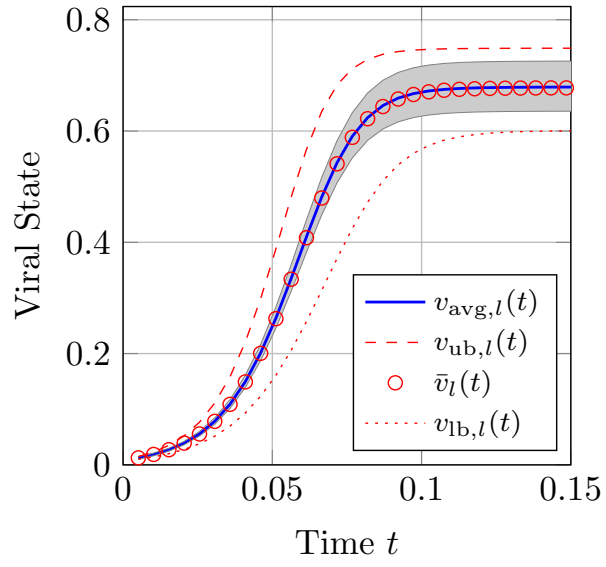

(c) Cell $\mathcal{N}_1$ and relative variance $\sigma_{\mathrm{rel}} = 0.5$.

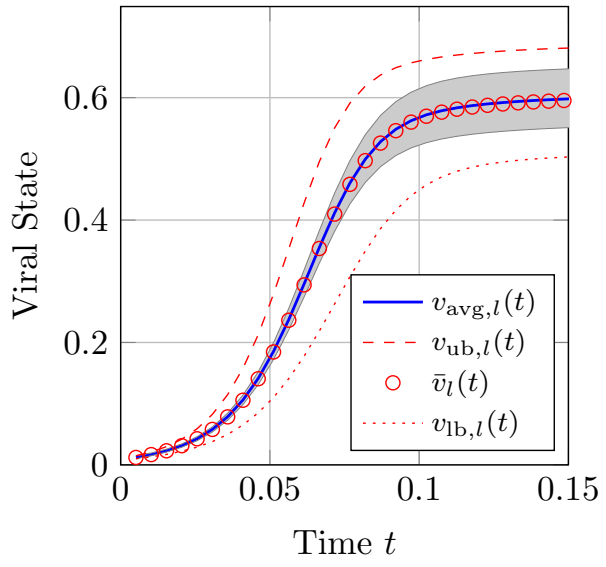

(d) Cell $\mathcal{N}_5$ and relative variance $\sigma_{\mathrm{rel}} = 0.5$.

Figure 5: **Low-dimensional approximation of the viral state dynamics.** For a stochastic blockmodel network with $N = 1000$ nodes and $r = 5$ cells, the accuracy of the approximation $\bar{v}_l(t)$ and the tightness of the bounds $v_{\mathrm{lb},l}(t)$, $v_{\mathrm{ub},l}(t)$ are depicted. The reduced-size viral states $\bar{v}(t)$,$v_{\mathrm{lb}}(t)$ and $v_{\mathrm{ub}}(t)$ are equal to the linear combination of $m = r = 5$ agitation modes y_l, each of which corresponds to one cell. **(a,b)**: The first row correspond to the relative variance $\sigma_{\mathrm{rel}} = 0.25$. **(c,d)**: The second row correspond to the relative variance $\sigma_{\mathrm{rel}} = 0.5$. **(a,c)**: The left column corresponds to the largest cell $\mathcal{N}_1$. **(b,d)**: The right column corresponds to the smallest cell $\mathcal{N}_5$. The viral state $v_i(t)$ of every node i in the respective cell $\mathcal{N}_l$ is within the shaded grey area.

The accuracy of the bounds $v_{\mathrm{lb},l}(t)$, $v_{\mathrm{ub},l}(t)$ on any viral state $v_i(t)$ in cell $\mathcal{N}_l$ decreases when the variance σ_{rel} is increased. Nonetheless, the bounds $v_{\mathrm{lb},l}(t)$, $v_{\mathrm{ub},l}(t)$ are reasonably accurate for both $\sigma_{\mathrm{rel}} = 0.25$ and $\sigma_{\mathrm{rel}} = 0.5$.

4.1 Clustering for epidemics on real-world networks

Approximating the viral state dynamics by $m < N$ equations requires the specification of a partition π of the nodes. In some cases, this partition is given *a priori*, as in the experiments in Figure 5, where the node partition π was chosen corresponding to the SBM blocks. In contrast, for real-world networks, it is more challenging to determine an appropriate clustering and, hence, to obtain an accurate description of the viral state dynamics by $m < N$ equations.

4.1.1 Bethe clustering

We consider a two-step approach to reduce NIMFA to $m = r < N$ equations. First, we obtain a partition π of the nodes by the Bethe spectral clustering algorithm [43], which makes use of the *Bethe Hessian* $H_\pm = (d_{\text{avg}} - 1)I \pm d_{\text{avg}}B + D$, with the average degree d_{avg} and the degree matrix $D = \text{diag}(d_1, ..., d_N)$. When the matrix B has an (approximate) SBM structure, the negative eigenvalues of $H_\pm$ have corresponding eigenvectors which are (approximately) piecewise constant on the blocks of B. The spectral clustering algorithm partitions the nodes of B based on a k-means clustering of the negative eigenvector entries of $H_\pm$. Second, we evaluate the accuracy of reduced-size viral state $\bar{v}(t)$ in (36) by the deviation of the prevalence,

$$\epsilon_{\text{avg}} = \sum_{k=1}^{n} \left| \frac{1}{N} \sum_{i=1}^{N} v_i\left(k\Delta t\right) - \frac{1}{N} \sum_{l=1}^{r} |\mathcal{N}_l| \, \bar{v}_l\left(k\Delta t\right) \right|. \tag{37}$$

Here, Δt denotes the sampling time, k is the discrete time, and the number of observations n is chosen such that the viral state $v(n\Delta t)$ practically converged to the steady state v_∞.

We applied the Bethe clustering algorithm to three real-world networks, which were accessed through [24]: the *American football* network [16] with $N = 115$ nodes and $L = 613$ links, for which $r = 10$ clusters were detected; the *primary school* contact network (day 1) [50] with $N = 236$ nodes and $L = 5899$ links, resulting in $r = 8$ clusters; and the *train bombing* network [18] with $N = 64$ nodes, $L = 243$ links and $r = 3$ identified clusters. For all networks, we considered homogeneous spreading rates β_{ij}, δ_i, which were set such that the basic reproduction number equals $R_0 = 3$. The initial viral state was set to $v_i(\Delta t) = 1/N$ for every node i. To evaluate the accuracy of the Bethe clustering approach, we additionally considered a collection of random partitions, which are obtained by randomly permuting the nodes in the partition π of the Bethe clustering.

Figure 6 shows that, for the football and the school network which have a clear community structure, the Bethe spectral clustering approach results in significantly more accurate low-dimensional viral dynamics $\bar{v}(t)$ than for random partitions. For the train network, which does not possess a clear community structure, there is a smaller advantage of Bethe clustering. Thus, our results indicate that if the network has an underlying community structure, then spectral clustering may be used to find an accurate low-dimensional approximation of the viral state dynamics.

Furthermore, for any partition π of the nodes, there are low-dimensional bounds $v_{\text{lb},l}(t)$, $v_{\text{ub},l}(t)$ of the viral state dynamics, as stated by Theorem 6. We define the errors ϵ_{ub} and ϵ_{lb} of the bounds $v_{\text{ub},l}(t)$ and $v_{\text{lb},l}(t)$ analogously to (37). Figure 7 demonstrates that the partition of the nodes by the Bethe clustering algorithm results in significantly more accurate lower bounds $v_{\text{lb},l}(t)$ than those obtained from random partitions, and somewhat more accurate upper bounds $v_{\text{ub},l}(t)$.

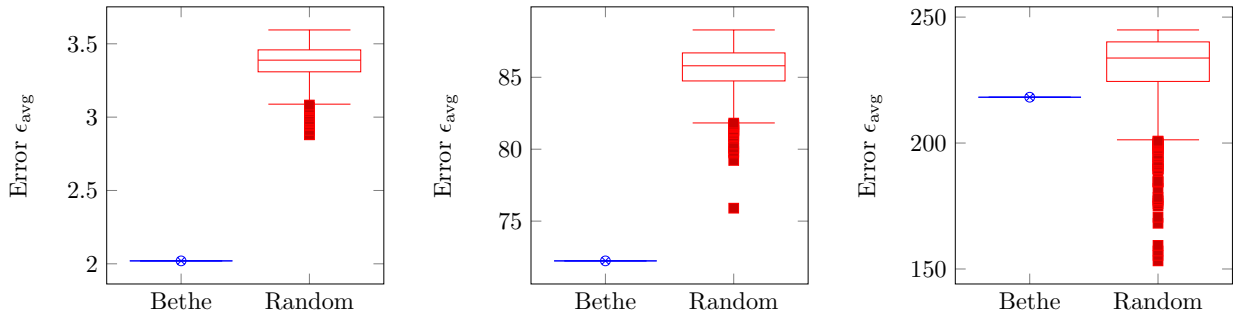

(a) American football. (b) Primary school. (c) Train bombing.

Figure 6: **Low-dimensional approximation of epidemics on real-world networks.** The error ϵ_{avg} of the reduced-size viral state $\bar{v}(t)$, in (36), for partitions obtained by Bethe clustering and random partitions. The accuracy is evaluated for three real-world networks: **(a)** American football network; **(b)** Primary school network; **(c)** Train bombing network.

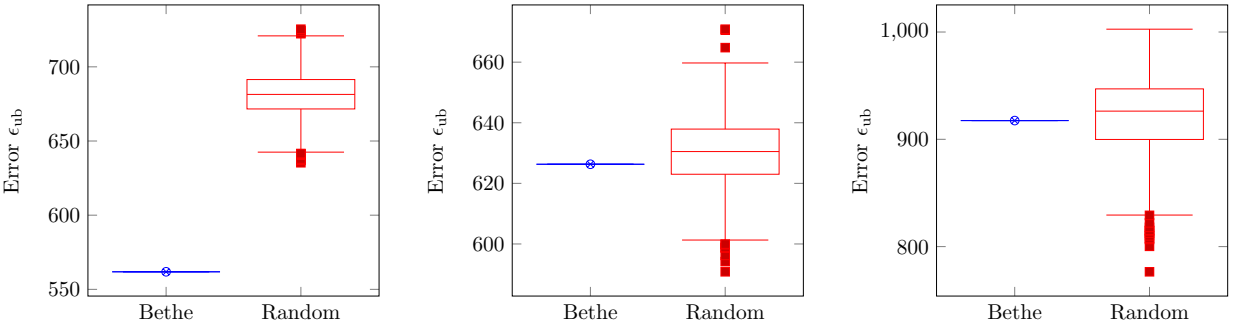

(a) American football. (b) Primary school. (c) Train bombing.

(d) American football. (e) Primary school. (f) Train bombing.

Figure 7: **Low-dimensional bounds of epidemics on real-world networks.** The errors of the low-dimensional bounds $v_{\text{lb},l}(t)$ and $v_{\text{ub},l}(t)$, stated by Theorem 6, for partitions obtained by Bethe clustering and random partitions. The subplots in the first and second row show the errors ϵ_{ub} and ϵ_{lb} of the upper bound $v_{\text{ub},l}(t)$ and the lower bound $v_{\text{ub},l}(t)$, respectively. The accuracy is evaluated for three real-world networks: **(a, d)** American football network; **(b, e)** Primary school network; **(c, f)** Train bombing network.

4.1.2 Cholera outbreak in London

We evaluate the NIMFA clustering method for the London Cholera outbreak in 1854. By mapping the Cholera deaths to individual households, Snow [49] argued that the spread of Cholera was due

to infected water of the Broad Street Pump, which was accessed by the majority of households. The dataset of Snow consists of $N = 251$ nodes. The nodes $i = 1, ..., 250$ correspond to households, and node $i = 251$ refers to the Broad Street Pump. Furthermore, the household $i = 208$ is a workhouse, whose residents had an own well and did not use the Broad Street Pump much. We follow the approach by Paré *et al.* [34, Matrix $A^{(3)}$] and set the elements of the 251×251 infection rate matrix B to

$$\beta_{ij} = \begin{cases} 1 & \text{if } \ i = j, \\ 1/10 & \text{if } \ j = 251, \ i = 208, \\ 1 & \text{if } \ j = 251, \ i \neq 208, \\ 0 & \text{otherwise.} \end{cases} \tag{38}$$

Thus, every household $i \neq 208$ is connected to the Broad Street Pump $j = 251$ with infection rate $\beta_{i,251} = 1$, except for the warehouse $i = 208$ whose limited access to the pump is considered by the lower infection rate $\beta_{208,251} = 1/10$. Furthermore, every household i has a unit-weight self-infection rate $\beta_{ii} = 1$, which accounts for the interaction of members within the same household. The curing rates δ_i are determined based on the fraction of Cholera deaths in household i. For more details on the data and modelling approach, we refer to [34].

We define the partition $\pi = \{\mathcal{N}_1, \mathcal{N}_2, \mathcal{N}_3\}$ with the cells $\mathcal{N}_1 = \{1, ..., 207, 209, ..., 250\}$, $\mathcal{N}_2 = \{208\}$ and $\mathcal{N}_3 = \{251\}$. For all cells $l, p = 1, 2, 3$, the sum of the infection rates $\sum_{k \in \mathcal{N}_l} \beta_{ik}$ and $\sum_{k \in \mathcal{N}_l} \beta_{ki}$ is the same for all nodes $i \in \mathcal{N}_p$. Hence, the partition π of the asymmetric matrix B is *inward equitable* and *outward equitable* [33], and the NIMFA viral dynamics could be reduced similarly to Theorem 1, which considered symmetric matrices B, provided the curing rates satisfy $\delta_i = \delta_j$ for all nodes i, j in any cell $\mathcal{N}_l$. However, the curing rates δ_i are not the same for all nodes $i \in \mathcal{N}_1$. Hence, Assumption 1 does not hold, and an *exact* reduction of the $N = 251$ NIMFA equations to $r = 3$ clusters is not possible.

Instead, we aim to *approximate* the $N = 251$ NIMFA equations by the reduced-size $r \times 1$ viral state $\bar{v}(t)$ in (36). Since the curing rates δ_i are not the same for all nodes $i \in \mathcal{N}_1$, we further partition the nodes in the cluster $\mathcal{N}_1$. More precisely, we obtain a partition $\mathcal{N}_{11}, \mathcal{N}_{12}, ..., \mathcal{N}_{1s}$ of the cluster $\mathcal{N}_1$ such that $\delta_i \approx \delta_j$ for all nodes $i, j \in \mathcal{N}_{1l}$, where $l = 1, ..., s$. We obtain the s clusters $\mathcal{N}_{11}, ..., \mathcal{N}_{1s}$ by the Matlab command `kmeans` applied to the curing rates δ_i, where $i \in \mathcal{N}_1$. Thus, in total there are $s + 2$ clusters $\mathcal{N}_{11}, ..., \mathcal{N}_{1s}, \mathcal{N}_2, \mathcal{N}_3$. We vary the number of subclusters from $s = 1$ to $s = 4$.

Figure 8 shows that the full-size NIMFA model with $N = 251$ nodes accurately captures the empirical data on the Cholera deaths, as already reported by [34]. Here, $v[k] = v(k\Delta t)$ and $\bar{v}[k] = \bar{v}(k\Delta t)$ denote the full-size and reduced-size viral states, respectively, at day k, and the discrete time step Δt equals one day. Figure 8a shows that clustering the nodes only based on the equitable partition $\pi = \{\mathcal{N}_1, \mathcal{N}_2, \mathcal{N}_3\}$ of the matrix B in (38) yields a reasonably accurate, reduced-size approximation of NIMFA with only $r = 3$ differential equations. The difference of reduced-size NIMFA to full-size NIMFA in Figure 8a is due to the different curing rates δ_i for nodes $i \in \mathcal{N}_1$. In Figure 8b the cell $\mathcal{N}_1$ is further partitioned into $s = 4$ cells $\mathcal{N}_{11}, ..., \mathcal{N}_{14}$, based on the curing rates δ_i. Then, the difference of reduced-size NIMFA to full-size NIMFA is negligible. Hence, we can describe the Cholera outbreak in London by the interaction of $r = 6$ clusters, given by the reduced-size system (36).

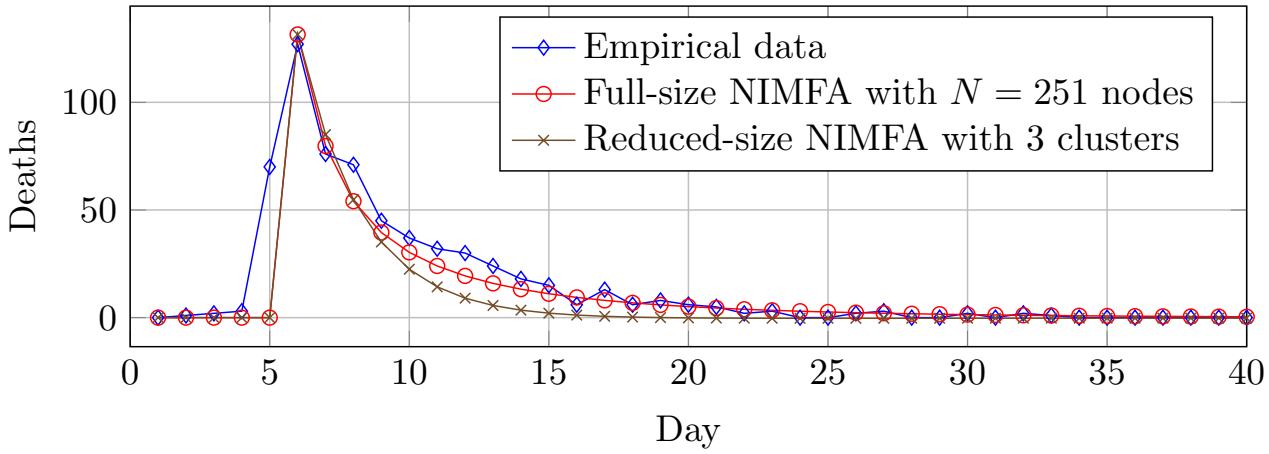

(a) Reduction to $r = 3$ clusters.

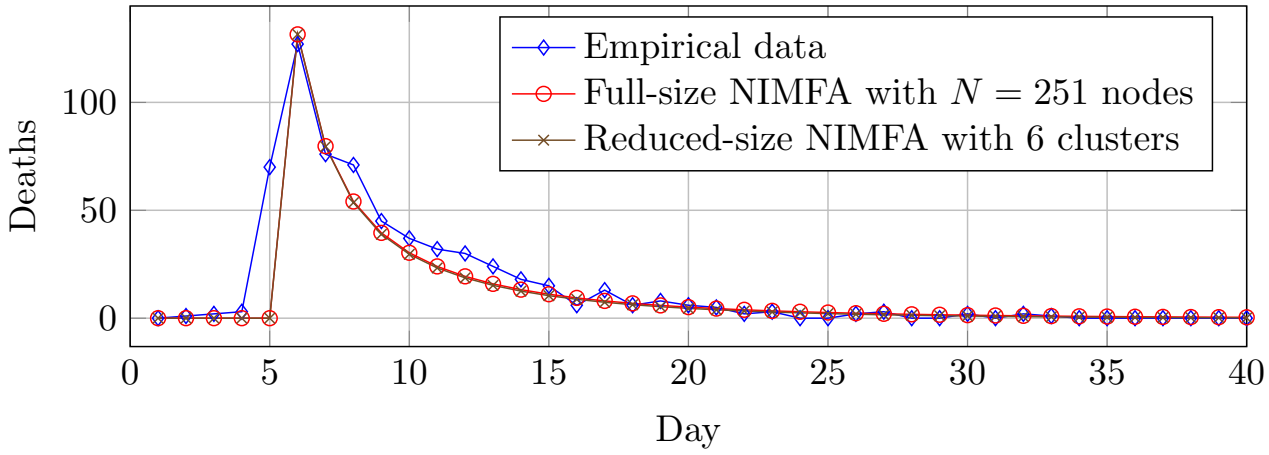

(b) Reduction to $r = 6$ clusters.

Figure 8: **Clustering NIMFA for the Cholera outbreak in London, 1854.** The blue curves show the daily Cholera deaths in London, gathered by Snow [49]. The red curve shows the change $y[k] - y[k-1]$ in the prevalence $y[k] = \sum_{i=1}^{N} v_i[k]$ of the NIMFA epidemic model versus day k. The NIMFA parameters were set in accordance to Paré *et al.* [34]. The brown curve shows the prevalence $\bar{y}[k] = \sum_{l=1}^{r} \bar{v}_r[k]$ of the reduced-size NIMFA model with: **(a)** $r = 3$ clusters, for which the cell $\mathcal{N}_1$ is not further partitioned ($s = 1$); **(b)** $r = 6$ clusters, for which the cell $\mathcal{N}_1$ is partitioned into $s = 4$ clusters.

5 Conclusions

In this work, we focussed on reducing NIMFA on a network with N nodes to only $m << N$ differential equations. We believe that the geometric clustering approach outlined in this work can be applied to other dynamics on networks, particularly to general epidemic models [44, 39] and the class of dynamics in [51, 4, 26, 41]. Our contribution is composed of three parts. In the first part, we showed that the viral dynamics evolve on an m-dimensional subspace $\mathcal{V}$ *if and only if* the contact network has an equitable partition with $m_1 \leq m$ cells. Thus, low-dimensional viral state dynamics and the macroscopic structure of equitable partitions are equivalent.

In the second part, we focussed on equitable partitions π with the same spreading rates β_{ij} and δ_i for all nodes i, j in the same cell $\mathcal{N}_l$. We considered the decomposition of the viral state $v(t) = v_{\ker}(t)+\tilde{v}(t)$ into two parts: the term $\tilde{v}(t)$ describes the viral state average in every cell $\mathcal{N}_l$; and the term $v_{\ker}(t)$ equals the projection of the viral state $v(t)$ onto the kernel of the infection rate matrix B. By showing that the term $\tilde{v}(t)$ evolves independently from the projection $v_{\ker}(t)$ and the projection $v_{\ker}(t)$ obeys a linear time-varying system, we derived the solution of the NIMFA differential equations on the complete graph for *arbitrary* initial conditions $v(0)$.

Strictly speaking, most contact networks do not have an equitable partition, and an exact reduction of the number of NIMFA equations is not possible. In the third part, we considered arbitrary contact networks with a (not necessarily equitable) partition of the nodes into m cells. For any partition of the nodes, we derived bounds and approximations of the NIMFA epidemics with only m differential equations. The "more equitable" the partition, the more accurate the approximation. Thus, finding (almost) equitable partitions is crucial for reducing an epidemic outbreak in a large population to the interaction of only few groups of individuals.

Acknowledgements

We are grateful to Philip E. Paré for providing the data on the Cholera outbreak in London. Furthermore, we are grateful to Massimo Achterberg and Qiang Liu for helpful discussions on this material.

Data Availability

The data that support the findings of this study are available from the corresponding author upon reasonable request.

References

[1] E. Abbe, "Community detection and stochastic block models: recent developments," *The Journal of Machine Learning Research*, vol. 18, no. 1, pp. 6446–6531, 2017.

[2] M. Abramowitz and I. A. Stegun, *Handbook of mathematical functions: with formulas, graphs, and mathematical tables*. Courier Corporation, 1965, vol. 55.

[3] A. Arenas, A. Diaz-Guilera, and C. J. Pérez-Vicente, "Synchronization reveals topological scales in complex networks," *Physical Review Letters*, vol. 96, no. 11, p. 114102, 2006.

[4] B. Barzel and A.-L. Barabási, "Universality in network dynamics," *Nature Physics*, vol. 9, no. 10, p. 673, 2013.

[5] S. Bonaccorsi, S. Ottaviano, D. Mugnolo, and F. D. Pellegrini, "Epidemic outbreaks in networks with equitable or almost-equitable partitions," *SIAM Journal on Applied Mathematics*, vol. 75, no. 6, pp. 2421–2443, 2015.

[6] S. L. Brunton and J. N. Kutz, *Data-driven science and engineering: Machine learning, dynamical systems, and control*. Cambridge University Press, 2019.

[7] A. Clauset, C. Moore, and M. E. Newman, "Hierarchical structure and the prediction of missing links in networks," *Nature*, vol. 453, no. 7191, pp. 98–101, 2008.

[8] V. Colizza, R. Pastor-Satorras, and A. Vespignani, "Reaction–diffusion processes and metapopulation models in heterogeneous networks," *Nature Physics*, vol. 3, no. 4, pp. 276–282, 2007.

[9] V. Colizza and A. Vespignani, "Epidemic modeling in metapopulation systems with heterogeneous coupling pattern: Theory and simulations," *Journal of Theoretical Biology*, vol. 251, no. 3, pp. 450–467, 2008.

[10] G. F. de Arruda, E. Cozzo, T. P. Peixoto, F. A. Rodrigues, and Y. Moreno, "Disease localization in multilayer networks," *Physical Review X*, vol. 7, no. 1, p. 011014, 2017.

[11] K. Devriendt and P. Van Mieghem, "Unified mean-field framework for Susceptible-Infected-Susceptible epidemics on networks, based on graph partitioning and the isoperimetric inequality," *Physical Review E*, vol. 96, no. 5, p. 052314, 2017.

[12] K. Devriendt and R. Lambiotte, "Nonlinear network dynamics with consensus–dissensus bifurcation," *Journal of Nonlinear Science*, vol. 31, no. 1, pp. 1–34, 2021.

[13] M. Egerstedt, S. Martini, M. Cao, K. Camlibel, and A. Bicchi, "Interacting with networks: How does structure relate to controllability in single-leader, consensus networks?" *IEEE Control Systems Magazine*, vol. 32, no. 4, pp. 66–73, 2012.

[14] R. S. Ferreira, R. Da Costa, S. Dorogovtsev, and J. F. F. Mendes, "Metastable localization of diseases in complex networks," *Physical Review E*, vol. 94, no. 6, p. 062305, 2016.

[15] S. Friedberg, A. Insel, and L. Spence, *Linear Algebra*. Prentice Hall, 1989.

[16] M. Girvan and M. E. Newman, "Community structure in social and biological networks," *Proceedings of the National Academy of Sciences*, vol. 99, no. 12, pp. 7821–7826, 2002.

[17] A. V. Goltsev, S. N. Dorogovtsev, J. G. Oliveira, and J. F. Mendes, "Localization and spreading of diseases in complex networks," *Physical Review Letters*, vol. 109, no. 12, p. 128702, 2012.

[18] B. Hayes, "Connecting the dots," *American Scientist*, vol. 94, no. 5, pp. 400–404, 2006.

[19] Z. He and P. Van Mieghem, "Prevalence expansion in nimfa," *Physica A: Statistical Mechanics and its Applications*, vol. 540, p. 123220, 2020.

[20] P. W. Holland, K. B. Laskey, and S. Leinhardt, "Stochastic blockmodels: First steps," *Social Networks*, vol. 5, no. 2, pp. 109–137, 1983.

[21] E. Kamke, "Zur Theorie der Systeme gewöhnlicher Differentialgleichungen. II." *Acta Mathematica*, vol. 58, pp. 57–85, 1932.

[22] I. Z. Kiss, J. C. Miller, and P. L. Simon, "Mathematics of epidemics on networks," *Cham: Springer*, vol. 598, 2017.

[23] A. L. Krause, L. Kurowski, K. Yawar, and R. A. Van Gorder, "Stochastic epidemic metapopulation models on networks: SIS dynamics and control strategies," *Journal of Theoretical Biology*, vol. 449, pp. 35–52, 2018.

[24] J. Kunegis, "Konect: the Koblenz network collection," in *Proceedings of the 22nd International Conference on World Wide Web*. ACM, 2013, pp. 1343–1350.

[25] A. Lajmanovich and J. A. Yorke, "A deterministic model for gonorrhea in a nonhomogeneous population," *Mathematical Biosciences*, vol. 28, no. 3-4, pp. 221–236, 1976.

[26] E. Laurence, N. Doyon, L. J. Dubé, and P. Desrosiers, "Spectral dimension reduction of complex dynamical networks," *Physical Review X*, vol. 9, no. 1, p. 011042, 2019.

[27] F. Liu, S. Cui, X. Li, and M. Buss, "On the stability of the endemic equilibrium of a discrete-time networked epidemic model," *arXiv preprint arXiv:2001.07451*, 2020.

[28] Q. Liu and P. Van Mieghem, "Network localization is unalterable by infections in bursts," *IEEE Transactions on Network Science and Engineering*, vol. 6, no. 4, pp. 983–989, 2018.

[29] D. Mugnolo, *Semigroup methods for evolution equations on networks*. Springer, 2014, vol. 20, no. 4.

[30] M. Müller, "Über das Fundamentaltheorem in der Theorie der gewöhnlichen Differentialgleichungen," *Mathematische Zeitschrift*, vol. 26, no. 1, pp. 619–645, 1927.

[31] C. Nowzari, V. M. Preciado, and G. J. Pappas, "Analysis and control of epidemics: A survey of spreading processes on complex networks," *IEEE Control Systems Magazine*, vol. 36, no. 1, pp. 26–46, 2016.

[32] N. O'Clery, Y. Yuan, G.-B. Stan, and M. Barahona, "Observability and coarse graining of consensus dynamics through the external equitable partition," *Physical Review E*, vol. 88, no. 4, p. 042805, 2013.

[33] S. Ottaviano, F. De Pellegrini, S. Bonaccorsi, and P. Van Mieghem, "Optimal curing policy for epidemic spreading over a community network with heterogeneous population," *Journal of Complex Networks*, vol. 6, no. 5, pp. 800–829, 2018.

[34] P. E. Paré, J. Liu, C. L. Beck, B. E. Kirwan, and T. Başar, "Analysis, estimation, and validation of discrete-time epidemic processes," *IEEE Transactions on Control Systems Technology*, vol. 28, no. 1, pp. 79–93, 2018.

[35] R. Pastor-Satorras, C. Castellano, P. Van Mieghem, and A. Vespignani, "Epidemic processes in complex networks," *Reviews of Modern Physics*, vol. 87, no. 3, pp. 925—-979, 2015.

[36] R. Pastor-Satorras and A. Vespignani, "Epidemic spreading in scale-free networks," *Physical review letters*, vol. 86, no. 14, p. 3200, 2001.

[37] L. M. Pecora, F. Sorrentino, A. M. Hagerstrom, T. E. Murphy, and R. Roy, "Cluster synchronization and isolated desynchronization in complex networks with symmetries," *Nature Communications*, vol. 5, no. 1, pp. 1–8, 2014.

[38] T. P. Peixoto, "Hierarchical block structures and high-resolution model selection in large networks," *Physical Review X*, vol. 4, no. 1, p. 011047, 2014.

[39] B. Prasse and P. Van Mieghem, "Network reconstruction and prediction of epidemic outbreaks for general group-based compartmental epidemic models," *IEEE Transactions on Network Science and Engineering*, 2020.

[40] ——, "The viral state dynamics of the discrete-time NIMFA epidemic model," *IEEE Transactions on Network Science and Engineering*, 2019.

[41] ——, "Predicting dynamics on networks hardly depends on the topology," *arXiv preprint arXiv:2005.14575*, 2020.

[42] ——, "Time-dependent solution of the NIMFA equations around the epidemic threshold," *Journal of Mathematical Biology*, vol. 81, no. 6, pp. 1299–1355, 2020.

[43] A. Saade, F. Krzakala, and L. Zdeborová, "Spectral clustering of graphs with the Bethe Hessian," in *Advances in Neural Information Processing Systems*, Z. Ghahramani, M. Welling, C. Cortes, N. Lawrence, and K. Q. Weinberger, Eds., vol. 27. Curran Associates, Inc., 2014. [Online]. Available: http://papers.nips.cc/paper/5520-spectral-clustering-of-graphs-with-the-bethehessian.pdf

[44] F. D. Sahneh, C. Scoglio, and P. Van Mieghem, "Generalized epidemic mean-field model for spreading processes over multilayer complex networks," *IEEE/ACM Transactions on Networking (TON)*, vol. 21, no. 5, pp. 1609–1620, 2013.

[45] M. T. Schaub, N. O'Clery, Y. N. Billeh, J.-C. Delvenne, R. Lambiotte, and M. Barahona, "Graph partitions and cluster synchronization in networks of oscillators," *Chaos: An Interdisciplinary Journal of Nonlinear Science*, vol. 26, no. 9, p. 094821, 2016.

[46] M. T. Schaub and L. Peel, "Hierarchical community structure in networks," *arXiv preprint arXiv:2009.07196*, 2020.

[47] A. J. Schwenk, "Computing the characteristic polynomial of a graph," in *Graphs and Combinatorics*. Springer, 1974, pp. 153–172.

[48] P. L. Simon, M. Taylor, and I. Z. Kiss, "Exact epidemic models on graphs using graph-automorphism driven lumping," *Journal of Mathematical Biology*, vol. 62, no. 4, pp. 479–508, 2011.

[49] J. Snow, *On the mode of communication of cholera*. John Churchill, 1855.

[50] J. Stehlé, N. Voirin, A. Barrat, C. Cattuto, L. Isella, J. Pinton, M. Quaggiotto, W. Van den Broeck, C. Régis, B. Lina, and P. Vanhems, "High-resolution measurements of face-to-face contact patterns in a primary school," *PLOS ONE*, vol. 6, no. 8, p. e23176, 08 2011. [Online]. Available: http://dx.doi.org/10.1371/journal.pone.0023176

[51] M. Timme, "Revealing network connectivity from response dynamics," *Physical Review Letters*, vol. 98, no. 22, p. 224101, 2007.

[52] P. Van den Driessche and J. Watmough, "Reproduction numbers and sub-threshold endemic equilibria for compartmental models of disease transmission," *Mathematical Biosciences*, vol. 180, no. 1-2, pp. 29–48, 2002.

[53] P. Van Mieghem, "SIS epidemics with time-dependent rates describing ageing of information spread and mutation of pathogens," *Delft University of Technology*, vol. 1, no. 15, 2014.

[54] P. Van Mieghem and J. Omic, "In-homogeneous virus spread in networks," *arXiv preprint arXiv:1306.2588*, 2014.

[55] P. Van Mieghem and R. Van de Bovenkamp, "Non-Markovian infection spread dramatically alters the susceptible-infected-susceptible epidemic threshold in networks," *Physical Review Letters*, vol. 110, no. 10, p. 108701, 2013.

[56] P. Van Mieghem, *Graph spectra for complex networks*. Cambridge University Press, 2010.

[57] ——, "The N-Intertwined SIS epidemic network model," *Computing*, vol. 93, no. 2-4, pp. 147–169, 2011.

[58] ——, "The viral conductance of a network," *Computer Communications*, vol. 35, no. 12, pp. 1494–1506, 2012.

[59] ——, *Performance Analysis of Complex Networks and Systems*. Cambridge University Press, 2014.

[60] P. Van Mieghem, J. Omic, and R. Kooij, "Virus spread in networks," *IEEE/ACM Transactions on Networking*, vol. 17, no. 1, pp. 1–14, 2009.

[61] J. A. Ward and M. López-García, "Exact analysis of summary statistics for continuous-time discrete-state Markov processes on networks using graph-automorphism lumping," *Applied Network Science*, vol. 4, no. 1, p. 108, 2019.

A Proof of Lemma 1

Let w denote a vector in the orthogonal complement $\mathcal{V}^\perp$ of the invariant set $\mathcal{V}$. Hence, it must hold that $w^T v(t) = 0$ for every time $t \geq 0$ if $v(0) \in \mathcal{V}$, which is equivalent to both $w^T v(0) = 0$ and

$$\frac{d(w^T v(t))}{dt} = 0 \quad \forall v(t) \in \mathcal{V}, w \in \mathcal{V}^\perp. \tag{A1}$$

We replace the notation $v(t) \in \mathcal{V}$ by $v \in \mathcal{V}$. Then, we obtain from the NIMFA equations (2) that (A1) is equivalent to

$$w^T \left(-Sv + \operatorname{diag}(u - v)Bv\right) = 0 \quad \forall v \in \mathcal{V}, w \in \mathcal{V}^\perp.$$

Under Assumption 1, it holds that $Sv \in \mathcal{V}$. Hence, the vector $w \in \mathcal{V}^\perp$ is orthogonal to the vector Sv, which yields that

$$w^T \operatorname{diag}(u - v)Bv = 0.$$

Since $\operatorname{diag}(u)$ is the identity matrix, we obtain that

$$w^T Bv = w^T \operatorname{diag}(v)Bv. \tag{A2}$$

Since the invariant set $\mathcal{V}$ is a subspace of $\mathbb{R}^N$, $v \in \mathcal{V}$ implies that $\gamma v \in \mathcal{V}$ for any scalar $\gamma \in \mathbb{R}$. For the vector γv, where we consider $\gamma > 0$, it follows from (A2) that

$$\gamma w^T Bv = \gamma^2 w^T \operatorname{diag}(v)Bv,$$

which is equivalent to

$$w^T Bv = \gamma w^T \operatorname{diag}(v)Bv.$$

Thus, we obtain with (A2) for every scalar $\gamma > 0$ that

$$w^T \operatorname{diag}(v)Bv = \gamma w^T \operatorname{diag}(v)Bv,$$

which implies that

$$w^T \operatorname{diag}(v)Bv = 0. \tag{A3}$$

Then, from (A2), it follows that

$$w^T Bv = 0$$

for all vectors $w \in \mathcal{V}^\perp$, $v \in \mathcal{V}$. The vector Bv is orthogonal to all vectors $w \in \mathcal{V}^\perp$, only if $Bv \in \mathcal{V}$. Thus, the set $\mathcal{V}$ is an invariant subspace [15] of the infection rate matrix B. The sets of vectors $y_1, ..., y_m$ and $y_{m+1}, ..., y_N$ span the invariant set $\mathcal{V}$ and the orthogonal complement $\mathcal{V}^\perp$, respectively, see (6) and (18). Thus, we can express the symmetric matrix B as

$$B = \begin{pmatrix} y_1 & ... & y_N \end{pmatrix} \begin{pmatrix} M_1 & M_{12} \\ 0 & M_2 \end{pmatrix} \begin{pmatrix} y_1^T \\ \vdots \\ y_N^T \end{pmatrix} \tag{A4}$$

for some $m \times m$ symmetric matrix M_1 and some $(N-m) \times (N-m)$ symmetric matrix M_2. The $m \times (N-m)$ matrix M_{12} describes the mapping from the subspace $\mathcal{V}^\perp$ to the subspace $\mathcal{V}$. Since the matrix B is symmetric, it holds that $M_{12} = 0$, and (A4) becomes

$$B = \begin{pmatrix} y_1 & ... & y_N \end{pmatrix} \begin{pmatrix} M_1 & 0 \\ 0 & M_2 \end{pmatrix} \begin{pmatrix} y_1^T \\ \vdots \\ y_N^T \end{pmatrix}.$$

Furthermore, since the matrix B is diagonalisable as (20), the matrices M_1 and M_2 are diagonalisable [15, Exercise 24, Section 5.4]. Thus, there is some orthogonal $m \times m$ matrix C_1 and some orthogonal $(N-m) \times (N-m)$ matrix C_2 such that

$$B = \begin{pmatrix} y_1 & ... & y_N \end{pmatrix} \begin{pmatrix} C_1 & 0 \\ 0 & C_2 \end{pmatrix} \begin{pmatrix} \Lambda_1 & 0 \\ 0 & \Lambda_2 \end{pmatrix} \begin{pmatrix} C_1^T & 0 \\ 0 & C_2^T \end{pmatrix} \begin{pmatrix} y_1^T \\ \vdots \\ y_N^T \end{pmatrix}. \tag{A5}$$

where the $m \times m$ diagonal matrix Λ_1 and the $(N-m) \times (N-m)$ diagonal matrix Λ_2 contain the eigenvalues of B. In contrast to the $N \times N$ matrix Λ in (20), the diagonal entries of the matrices Λ_1 and Λ_2 may not be ordered with respect to their magnitude. Hence, there is some permutation $\phi : \{1, ..., N\} \to \{1, ..., N\}$ of the eigenvalues $\lambda_1, ..., \lambda_N$ such that

$$\Lambda_1 = \operatorname{diag}\left(\lambda_{\phi(1)}, ..., \lambda_{\phi(m)}\right)$$

and

$$\Lambda_2 = \operatorname{diag}\left(\lambda_{\phi(m+1)}, ..., \lambda_{\phi(N)}\right).$$

We define the $N \times m$ matrix $E_\mathcal{V}$ and the $N \times (N-m)$ matrix $E_{\mathcal{V}^\perp}$ as

$$E_\mathcal{V} = \begin{pmatrix} y_1 & ... & y_m \end{pmatrix} C_1$$

and

$$E_{\mathcal{V}^\perp} = \begin{pmatrix} y_{N-m} & ... & y_N \end{pmatrix} C_2.$$

Since the matrices C_1 and C_2 are nonsingular, the columns of the matrices $E_\mathcal{V}$ and $E_{\mathcal{V}^\perp}$ span the subspaces $\mathcal{V}$ and $\mathcal{V}^\perp$, respectively. We obtain that

$$B = \begin{pmatrix} E_\mathcal{V} & E_{\mathcal{V}^\perp} \end{pmatrix} \operatorname{diag}\left(\lambda_{\phi(1)}, ..., \lambda_{\phi(N)}\right) \begin{pmatrix} E_\mathcal{V}^T \\ E_{\mathcal{V}^\perp}^T \end{pmatrix}.$$

Thus, the matrices $E_{\mathcal{V}}, E_{\mathcal{V}^\perp}$ are equal to

$$E_{\mathcal{V}} = \begin{pmatrix} x_{\phi(1)} & ... & x_{\phi(m)} \end{pmatrix} \tag{A6}$$

and

$$E_{\mathcal{V}^\perp} = \begin{pmatrix} x_{\phi(N-m)} & ... & x_{\phi(N)} \end{pmatrix},$$

where the columns $x_{\phi(1)}, ..., x_{\phi(N)}$ are eigenvectors to the eigenvalues $\lambda_{\phi(1)}, ..., \lambda_{\phi(N)}$ of the matrix B, which completes the proof.

B Proof of Lemma 2

From (A5), it follows that

$$B = \begin{pmatrix} y_1 & ... & y_m \end{pmatrix} C_1 \Lambda_1 C_1^T \begin{pmatrix} y_1^T \\ \vdots \\ y_m^T \end{pmatrix} + \begin{pmatrix} y_{m+1} & ... & y_N \end{pmatrix} C_2 \Lambda_2 C_2^T \begin{pmatrix} y_{m+1}^T \\ \vdots \\ y_N^T \end{pmatrix}.$$

We complete the proof by identifying the $m \times m$ matrix $\tilde{B}_{\mathcal{V}} = C_1 \Lambda_1 C_1^T$ and the $(N-m) \times (N-m)$ matrix $\tilde{B}_{\mathcal{V}^\perp} = C_2 \Lambda_2 C_2^T$.

C Proof of Theorem 2

The proof of Theorem 2 is based on four lemmas. First, Lemma 3 relates the product $\operatorname{diag}(w)v$ to the subspaces $\mathcal{V}_{\neq 0}$ and $\mathcal{V}^\perp$:

Lemma 3. *For all vectors $v \in \mathcal{V}_{\neq 0}$ and $w \in \mathcal{V}^\perp$, it holds that* $\operatorname{diag}(w)v \in \mathcal{V}^\perp$.

Proof. Since $w^T \operatorname{diag}(v) = (w_1 v_1, ..., w_N v_N) = v^T \operatorname{diag}(w)$, we obtain from (A3) that

$$v^T \operatorname{diag}(w) B v = 0.$$

Equivalently, by taking the transpose, it holds that

$$v^T B \operatorname{diag}(w) v = 0. \tag{C1}$$

The invariant set $\mathcal{V}$ is given by the span of some orthogonal vectors $y_1, ..., y_m$. By Lemma 1, it holds that $\mathcal{V} = \operatorname{span}\{x_{\phi(1)}, ..., x_{\phi(m)}\}$, where $x_{\phi(l)}$ is an eigenvector of the matrix B to the eigenvalue $\lambda_{\phi(l)}$ for some permutation ϕ. Thus, every vector $v \in \mathcal{V}$ can be written as

$$v = \begin{pmatrix} x_{\phi(1)} & ... & x_{\phi(m)} \end{pmatrix} z \tag{C2}$$

for some $m \times 1$ vector $z = (z_1, ..., z_m)^T$, and the subspace $\mathcal{V}$ equals

$$\mathcal{V} = \left\{ \begin{pmatrix} x_{\phi(1)} & ... & x_{\phi(m)} \end{pmatrix} z \middle| z \in \mathbb{R}^m \right\}.$$

With (C2), we can rewrite (C1) as

$$z^T \Lambda_1 \begin{pmatrix} x_{\phi(1)}^T \\ \vdots \\ x_{\phi(m)}^T \end{pmatrix} \operatorname{diag}(w) \begin{pmatrix} x_{\phi(1)} & ... & x_{\phi(m)} \end{pmatrix} z = 0, \tag{C3}$$

with the $m \times m$ diagonal matrix $\Lambda_1 = \operatorname{diag}(\lambda_{\phi(1)}, ..., \lambda_{\phi(m)})$. The quadratic form (C3) equals zero for all vectors $cz \in \mathbb{R}^m$ if and only if

$$\Lambda_1 \begin{pmatrix} x_{\phi(1)}^T \\ \vdots \\ x_{\phi(m)}^T \end{pmatrix} \operatorname{diag}(w) \begin{pmatrix} x_{\phi(1)} & ... & x_{\phi(m)} \end{pmatrix} = 0,$$

which implies, with (C2), that

$$\Lambda_1 \begin{pmatrix} x_{\phi(1)}^T \\ \vdots \\ x_{\phi(m)}^T \end{pmatrix} \operatorname{diag}(w) v = 0$$

for all vectors $v \in \mathcal{V}$. Componentwise, we obtain that

$$\lambda_{\phi(l)} x_{\phi(l)}^T \operatorname{diag}(w) v = 0 \tag{C4}$$

for all rows $l = 1, ..., m$ and all vectors $v \in \mathcal{V}$. Equation (C4) is satisfied if and only if $\lambda_{\phi(l)} = 0$ or $x_{\phi(l)}^T \operatorname{diag}(w) v = 0$ for all rows $l = 1, ..., m$. The subspace $\mathcal{V}_0$ contains the vectors $x_{\phi(l)}$ for which $\lambda_{\phi(l)} = 0$, and the subspace $\mathcal{V}^\perp$ contains the vectors $x_{\phi(m+1)}, ..., x_{\phi(N)}$ which are orthogonal to the vectors $x_{\phi(1)}, ..., x_{\phi(m)}$. Thus, the vector $\operatorname{diag}(w) v$ must be element of the subspaces $\mathcal{V}_0$ or $\mathcal{V}^\perp$, or the vector $\operatorname{diag}(w) v$ must be equal to the sum of two vectors in the subspaces $\mathcal{V}_0$ and $\mathcal{V}$. Hence, with the direct sum (19), we can reformulate (C4) as

$$\operatorname{diag}(w) v \in \mathcal{V}^\perp \oplus \mathcal{V}_0 \tag{C5}$$

for all vectors $v \in \mathcal{V}$. We define the $N \times m_1$ matrix $E_{\mathcal{V}_{\neq 0}}$ as

$$E_{\mathcal{V}_{\neq 0}} = \begin{pmatrix} x_{\phi(1)} & ... & x_{\phi(m_1)} \end{pmatrix}$$

and the $N \times (m - m_1)$ matrix $E_{\mathcal{V}_0}$ as

$$E_{\mathcal{V}_0} = \begin{pmatrix} x_{\phi(m_1+1)} & ... & x_{\phi(m)} \end{pmatrix}.$$

Thus, the definition of the matrix $E_{\mathcal{V}}$ in (A6) implies that $E_{\mathcal{V}} = \begin{pmatrix} E_{\mathcal{V}_{\neq 0}} & E_{\mathcal{V}_0} \end{pmatrix}$, and the matrix $\operatorname{diag}(w)$ can be written as

$$\operatorname{diag}(w) = \begin{pmatrix} E_{\mathcal{V}_{\neq 0}} & E_{\mathcal{V}_0} & E_{\mathcal{V}^\perp} \end{pmatrix} \begin{pmatrix} M_{11} & M_{12} & M_{13} \\ M_{21} & M_{22} & M_{23} \\ M_{31} & M_{32} & M_{33} \end{pmatrix} \begin{pmatrix} E_{\mathcal{V}_{\neq 0}}^T \\ E_{\mathcal{V}_0}^T \\ E_{\mathcal{V}^\perp}^T \end{pmatrix}$$

for some matrices M_{ij}, where $i, j = 1, 2, 3$, whose dimensions follow from the dimension of the matrices $E_{\mathcal{V}_{\neq 0}}$, $E_{\mathcal{V}_0}$ and $E_{\mathcal{V}^\perp}$. The matrices M_{11} and M_{12} describe the mapping of the matrix $\mathrm{diag}(w)$ from the subspaces $\mathcal{V}_{\neq 0}$ and $\mathcal{V}_0$, respectively, to the subspace $\mathcal{V}_{\neq 0}$. From (C5), we obtain that $M_{11} = 0$ and $M_{12} = 0$. Furthermore, since the matrix $\mathrm{diag}(w)$ is symmetric, it holds that $M_{21} = M_{12}^T = 0$. Hence, to satisfy (C5), the matrix $\mathrm{diag}(w)$ must be equal to

$$\mathrm{diag}(w) = \begin{pmatrix} E_{\mathcal{V}_{\neq 0}} & E_{\mathcal{V}_0} & E_{\mathcal{V}^\perp} \end{pmatrix} \begin{pmatrix} 0 & 0 & M_{13} \\ 0 & M_{22} & M_{23} \\ M_{31} & M_{32} & M_{33} \end{pmatrix} \begin{pmatrix} E_{\mathcal{V}_{\neq 0}}^T \\ E_{\mathcal{V}_0}^T \\ E_{\mathcal{V}^\perp}^T \end{pmatrix},$$

which implies for all vectors $v \in \mathcal{V}_{\neq 0}$ that $\mathrm{diag}(w)v \in \mathcal{V}^\perp$. □

Lemma 3 states that for all vectors $v \in \mathcal{V}_{\neq 0}$ and $w \in \mathcal{V}^\perp$, there must be some vector $\tilde{w} \in \mathcal{V}^\perp$ such that

$$\mathrm{diag}(w)v = \tilde{w}. \tag{C6}$$

We aim to find *all* subspaces $\mathcal{V}_{\neq 0}$ and $\mathcal{V}^\perp$ whose elements v and $w, \tilde{w}$, respectively, satisfy (C6). From Lemma 1 it follows that a basis of the $N - m$ dimensional subspace $\mathcal{V}^\perp$ is given by the columns of the matrix

$$E_{\mathcal{V}^\perp} = \begin{pmatrix} \left(x_{\phi(m+1)}\right)_1 & \dots & \left(x_{\phi(N)}\right)_1 \\ \vdots & \ddots & \vdots \\ \left(x_{\phi(m+1)}\right)_N & \dots & \left(x_{\phi(N)}\right)_N \end{pmatrix}. \tag{C7}$$

For every matrix, the column rank equals the row rank. Since the columns of the matrix $E_{\mathcal{V}^\perp}$ are linearly independent, there are $N - m$ linearly independent rows of the matrix $E_{\mathcal{V}^\perp}$. Without loss of generality[7], we assume that the *first* $N - m$ rows of the matrix $E_{\mathcal{V}^\perp}$ are linearly independent. Hence, the first $N - m$ rows span the Euclidean space $\mathbb{R}^{N-m}$,

$$\mathrm{span}\left\{ \begin{pmatrix} \left(x_{\phi(m+1)}\right)_1 \\ \vdots \\ \left(x_{\phi(N)}\right)_1 \end{pmatrix}, \begin{pmatrix} \left(x_{\phi(m+1)}\right)_2 \\ \vdots \\ \left(x_{\phi(N)}\right)_2 \end{pmatrix}, \dots, \begin{pmatrix} \left(x_{\phi(m+1)}\right)_{N-m} \\ \vdots \\ \left(x_{\phi(N)}\right)_{N-m} \end{pmatrix} \right\} = \mathbb{R}^{N-m}. \tag{C8}$$

Thus, for *all* vectors $w \in \mathcal{V}^\perp$ and $v \in \mathcal{V}_{\neq 0}$, there is a vector $\tilde{w} \in \mathcal{V}^\perp$ whose first $N - m$ entries satisfy (C6), i.e.,

$$\tilde{w}_i = w_i v_i, \quad i = 1, \dots, N - m. \tag{C9}$$

The last m entries of the vector $\tilde{w} \in \mathcal{V}^\perp$ are determined by the first $(N - m)$ entries of the vector w, as shown by Lemma 4. (Lemma 4 is not a novel contribution, but we include Lemma 4 for completeness.)

Lemma 4. *Suppose that that the first $N - m$ rows of the matrix $E_{\mathcal{V}^\perp}$ are linearly independent. Then, there are some $(N - m) \times 1$ vectors $\chi_{N-m}, \dots, \chi_N$ such that the last m entries of any vector $w \in \mathcal{V}^\perp$ follow from the first $(N - m)$ entries as*

$$w_i = \chi_i^T \begin{pmatrix} w_1 \\ \vdots \\ w_{N-m} \end{pmatrix}, \quad i = N - m + 1, \dots, N.$$

[7] Otherwise, consider a permutation of the rows, which is equivalent to a relabelling of the nodes.

Proof. With the definition of the matrix $E_{\mathcal{V}^\perp}$ in (C7), every vector $w \in \mathcal{V}^\perp$ can be written as

$$w = \begin{pmatrix} x_{\phi(m+1)} & \dots & x_{\phi(N)} \end{pmatrix} \begin{pmatrix} z_{m+1} \\ \vdots \\ z_N \end{pmatrix} \tag{C10}$$

for some scalars $z_{m+1}, ..., z_N \in \mathbb{R}$. Thus, the first $N-m$ entries of the vector w follow as

$$\begin{pmatrix} w_1 \\ \vdots \\ w_{N-m} \end{pmatrix} = M \begin{pmatrix} z_{m+1} \\ \vdots \\ z_N \end{pmatrix}, \tag{C11}$$

where the $(N-m) \times (N-m)$ matrix M equals the first $N-m$ rows of the matrix $E_{\mathcal{V}^\perp}$,

$$M = \begin{pmatrix} \left(x_{\phi(m+1)}\right)_1 & \dots & \left(x_{\phi(N)}\right)_1 \\ \vdots & \ddots & \vdots \\ \left(x_{\phi(m+1)}\right)_{N-m} & \dots & \left(x_{\phi(N)}\right)_{N-m} \end{pmatrix}.$$

By assumption, the first $N-m$ rows of the matrix $E_{\mathcal{V}^\perp}$ are linearly independent. Hence, the matrix M is nonsingular, and the scalars $z_{m+1}, ..., z_N$ follow from (C11) as

$$\begin{pmatrix} z_{m+1} \\ \vdots \\ z_N \end{pmatrix} = M^{-1} \begin{pmatrix} w_1 \\ \vdots \\ w_{N-m} \end{pmatrix}.$$

Thus, we obtain the last m entries of the vector w with (C10) as

$$\begin{aligned} \begin{pmatrix} w_{N-m+1} \\ \vdots \\ w_N \end{pmatrix} &= \begin{pmatrix} \left(x_{\phi(m+1)}\right)_{N-m+1} & \dots & \left(x_{\phi(N)}\right)_{N-m+1} \\ \vdots & \ddots & \vdots \\ \left(x_{\phi(m+1)}\right)_N & \dots & \left(x_{\phi(N)}\right)_N \end{pmatrix} \begin{pmatrix} z_{m+1} \\ \vdots \\ z_N \end{pmatrix} \\ &= \begin{pmatrix} \left(x_{\phi(m+1)}\right)_{N-m+1} & \dots & \left(x_{\phi(N)}\right)_{N-m+1} \\ \vdots & \ddots & \vdots \\ \left(x_{\phi(m+1)}\right)_N & \dots & \left(x_{\phi(N)}\right)_N \end{pmatrix} M^{-1} \begin{pmatrix} w_1 \\ \vdots \\ w_{N-m} \end{pmatrix}. \end{aligned}$$

To complete the proof, we define the vectors $\chi_{N-m+1}, ..., \chi_N$ as

$$\begin{pmatrix} \chi_{N-m+1}^T \\ \vdots \\ \chi_N^T \end{pmatrix} = \begin{pmatrix} \left(x_{\phi(m+1)}\right)_{N-m+1} & \dots & \left(x_{\phi(N)}\right)_{N-m+1} \\ \vdots & \ddots & \vdots \\ \left(x_{\phi(m+1)}\right)_N & \dots & \left(x_{\phi(N)}\right)_N \end{pmatrix} M^{-1}.$$

□

We combine Lemma 4 and (C9), which yields for the last $(N-m)$ entries of the vector $\tilde{w} \in \mathcal{V}^\perp$ that

$$\begin{aligned} \tilde{w}_i &= \sum_{j=1}^{N-m} \chi_{ij} \tilde{w}_j \\ &= \sum_{j=1}^{N-m} \chi_{ij} w_j v_j, \end{aligned}$$

where $i = N - m + 1, ..., N$. Furthermore, (C6) states that $\tilde{w}_i = v_i w_i$. Thus, it must hold that

$$w_i v_i = \sum_{j=1}^{N-m} \chi_{ij} w_j v_j$$

for the entries $i = N - m + 1, ..., N$. Since the vector w is element of the subspace $\mathcal{V}^\perp$, we apply Lemma 4 again and obtain that

$$\left(\sum_{j=1}^{N-m} \chi_{ij} w_j \right) v_i = \sum_{j=1}^{N-m} \chi_{ij} w_j v_j.$$

Thus, for all entries $i = N - m + 1, ..., N$, it must hold that

$$\sum_{j=1}^{N-m} \chi_{ij} w_j (v_i - v_j) = 0 \tag{C12}$$

for all vectors $w \in \mathcal{V}^\perp$ and $v \in \mathcal{V}_{\neq 0}$. Since the first $N - m$ rows of the matrix $E_{\mathcal{V}^\perp}$ are linearly independent, see (C8), it follows that (C12) must be satisfied for *all* scalars w_1, ..., w_{N-m} in $\mathbb{R}$. Hence, for all vectors $v \in \mathcal{V}_{\neq 0}$, it must hold that $\chi_{ij}(v_i - v_j) = 0$ for all indices $j = 1, ..., N - m$, which is equivalent to $\chi_{ij} = 0$ or $v_j = v_i$. Thus, the non-zero entries of the vectors χ_i indicate which nodes j have the same viral state as node i.

Example 5. *Consider a network of $N = 5$ nodes with an invariant set $\mathcal{V}$ of dimension $m = 3$. Furthermore, consider that $\mathcal{V}_0 = \emptyset$, which implies with (22) that $\mathcal{V} = \mathcal{V}_{\neq 0}$. Thus, there are $N - m = 2$ vectors χ_4, χ_5. Suppose that the vectors χ_4, χ_5 are equal to $\chi_4 = (\chi_{41}, 0)^T$ and $\chi_5 = (0, \chi_{52})^T$, where $\chi_{41}, \chi_{52} \neq 0$. Then, (C12) implies that $v_1 = v_4$ and $v_2 = v_5$ for every viral state $v \in \mathcal{V}$. Hence, the subspace $\mathcal{V} = \text{span}\{y_1, y_2, y_3\}$ is given by the basis vectors*

$$y_1 = \frac{1}{\sqrt{2}} \begin{pmatrix} 1 \\ 0 \\ 0 \\ 1 \\ 0 \end{pmatrix}, \quad y_2 = \frac{1}{\sqrt{2}} \begin{pmatrix} 0 \\ 1 \\ 0 \\ 0 \\ 1 \end{pmatrix}, \quad y_3 = \begin{pmatrix} 0 \\ 0 \\ 1 \\ 0 \\ 0 \end{pmatrix}.$$

For $l = 1, 2, 3$, the eigenvector $x_{\phi(l)}$ of the infection rate matrix B equals a linear combination of the basis vectors y_1, y_2, y_3.

From (C12), we can determine disjoint subsets $\mathcal{N}_1, \mathcal{N}_2, ...$ of the set of all nodes $\mathcal{N} = \{1, ..., N\}$ as follows: If two nodes i, j are element of the same subset $\mathcal{N}_l \subseteq \mathcal{N}$, then the viral states are equal, $v_i = v_j$, for every viral state $v \in \mathcal{V}_{\neq 0}$. If a subset contains only one node, $\mathcal{N}_l = \{i\}$, then the viral state can be arbitrary $v_i \in \mathbb{R}$, independently of the viral state v_j of other nodes $j \neq i$. Every subset defines a basis vector y_l of the subspace $\mathcal{V}_{\neq 0}$ as

$$(y_l)_i = \begin{cases} \frac{1}{\sqrt{|\mathcal{N}_l|}} & \text{if} \quad i \in \mathcal{N}_l, \\ 0 & \text{if} \quad i \notin \mathcal{N}_l. \end{cases} \tag{C13}$$

Then, the subspace $\mathcal{V}_{\neq 0}$ equals the span of the vectors y_l of all subsets $\mathcal{N}_l$. Since the dimension of the subspace $\mathcal{V}_{\neq 0}$ is m_1, there must be m_1 subsets $\mathcal{N}_1, ..., \mathcal{N}_{m_1}$. Every node i is element of at most one subset $\mathcal{N}_l$. Hence, the vectors $y_l, y_{\tilde{l}}$ are orthogonal for $l \neq \tilde{l}$.

Furthermore, some nodes i might not be element of any subset $\mathcal{N}_1, ..., \mathcal{N}_{m_1}$, which would imply that $(y_l)_i = 0$ for all basis vectors y_l of $\mathcal{V}_{\neq 0}$. We define the subset $\mathcal{N}_{m_1+1}$, whose elements are the nodes i that are not in any other subset $\mathcal{N}_1, ..., \mathcal{N}_{m_1}$. As shown by Lemma 5, the set $\mathcal{N}_{m_1+1}$ is empty:

Lemma 5. *Under Assumptions 1 to 4, it holds that* $\mathcal{N}_{m_1+1} = \emptyset$.

Proof. Under Assumption 2, there is a viral state vector $v \in \mathcal{V}$ with positive entries. The positive viral state vector v satisfies

$$v = \sum_{l=1}^{m_1} z_l y_l + \sum_{l=m_1+1}^{m} z_l y_l \tag{C14}$$

for some scalars $z_1, ..., z_m \in \mathbb{R}$. We denote the projection of the viral state v onto the subspace $\mathcal{V}_0$ as

$$v_{\text{ker}} = \sum_{l=m_1+1}^{m} z_l y_l$$

Every basis vector y_l of the subspace $\mathcal{V}_{\neq 0}$ satisfies $(y_l)_i = 0$ for all nodes $i \in \mathcal{N}_{m_1+1}$. Thus, we obtain with (C14) that

$$(v_{\text{ker}})_i = v_i > 0 \tag{C15}$$

for all nodes $i \in \mathcal{N}_{m_1+1}$. Any vector $\tilde{v} \in \mathcal{V}_{\neq 0}$ is orthogonal to the vector $v_{\text{ker}} \in \mathcal{V}_0$. Hence, it holds that

$$\sum_{i=1}^{N} (\tilde{v})_i (v_{\text{ker}})_i = 0.$$

We split the sum

$$\sum_{l=1}^{m_1} \sum_{i \in \mathcal{N}_l} (\tilde{v})_i (v_{\text{ker}})_i + \sum_{i \in \mathcal{N}_{m_1+1}} (\tilde{v})_i (v_{\text{ker}})_i = 0.$$

Since $(\tilde{v})_i = 0$ for all nodes $i \in \mathcal{N}_{m_1+1}$, we obtain that

$$\sum_{l=1}^{m_1} \sum_{i \in \mathcal{N}_l} (\tilde{v})_i (v_{\text{ker}})_i = 0 \quad \forall \tilde{v} \in \mathcal{V}_{\neq 0}. \tag{C16}$$

Furthermore, we define the $N \times 1$ vector u_a with the entries

$$(u_a)_i = \begin{cases} 1 & \text{if } i \notin \mathcal{N}_{m_1+1}, \\ 0 & \text{if } i \in \mathcal{N}_{m_1+1}. \end{cases}$$

From the definition of the basis vectors y_l in (C13), it follows that the vector u_a equals

$$u_a = \sum_{l=1}^{m_1} \sqrt{|\mathcal{N}_l|} y_l.$$

Thus, vector u_a is element of $\mathcal{V}_{\neq 0}$. Since the vector v_{ker} is in the kernel of the matrix B, it holds that $Bv_{\text{ker}} = 0$, which implies that

$$u_a^T B v_{\text{ker}} = 0. \tag{C17}$$

We decompose the vector v_{ker} as $v_{\text{ker}} = v_{\text{ker},a} + v_{\text{ker},b}$, where the first addend equals

$$(v_{\text{ker},a})_i = \begin{cases} (v_{\text{ker}})_i & \text{if } i \notin \mathcal{N}_{m_1+1}, \\ 0 & \text{if } i \in \mathcal{N}_{m_1+1}, \end{cases}$$

and the second addend equals

$$(v_{\text{ker},b})_i = \begin{cases} 0 & \text{if } i \notin \mathcal{N}_{m_1+1} \\ (v_{\text{ker}})_i & \text{if } i \in \mathcal{N}_{m_1+1}. \end{cases} \tag{C18}$$

Then, (C17) becomes

$$u_a^T B v_{\text{ker},a} + u_a^T B v_{\text{ker},b} = 0.$$

Since $u_a \in \mathcal{V}_{\neq 0}$ and $\mathcal{V}_{\neq 0}$ is an invariant subspace of the matrix B, it holds that $Bu_a \in \mathcal{V}_{\neq 0}$. Thus, (C16) implies that $u_a^T B v_{\text{ker},a} = 0$, and we obtain that

$$u_a^T B v_{\text{ker},b} = 0,$$

which is equivalent to

$$\sum_{l=1}^{m_1} \sum_{i \in \mathcal{N}_l} \sum_{j=1}^{N} \beta_{ij} \left(v_{\text{ker},b}\right)_j = 0.$$

With the definition of the vector $v_{\text{ker},b}$ in (C18), we obtain that

$$\sum_{l=1}^{m_1} \sum_{i \in \mathcal{N}_l} \sum_{j \in \mathcal{N}_{m_1+1}} \beta_{ij} \left(v_{\text{ker}}\right)_j = 0. \tag{C19}$$

As stated by (C15), the entries $(v_{\text{ker}})_j$ are positive for all nodes $j \in \mathcal{N}_{m_1+1}$. Furthermore, the infection rates β_{ij} are non-negative under Assumption 3. Hence, (C19) is satisfied only if $\beta_{ij} = 0$ for all nodes $j \in \mathcal{N}_{m_1+1}$ and $i \in \mathcal{N}_l$ for all subsets $l = 1, ..., m_1$. In other words, the nodes in $\mathcal{N}_{m_1+1}$ are not connected to any nodes in $\mathcal{N}_1, ..., \mathcal{N}_{m_1}$, which contradicts the irreducibility of the matrix B under Assumption 4. Hence, it must hold that $\mathcal{N}_{m_1+1} = \emptyset$. □

Since $\mathcal{N}_{m_1+1} = \emptyset$, it holds that $\mathcal{N}_1 \cup ... \cup \mathcal{N}_{m_1} = \mathcal{N}$. Hence, the disjoint subsets $\mathcal{N}_1$, ..., $\mathcal{N}_{m_1}$ define a partition of the set of all nodes $\mathcal{N} = \{1, ..., N\}$. To complete the proof of Theorem 2, we must show that the subsets $\mathcal{N}_1$, ..., $\mathcal{N}_{m_1}$ are an *equitable* partition of the infection rate matrix B. Hence, we must show that the sum of the infection rates β_{ij},

$$\sum_{j \in \mathcal{N}_l} \beta_{ij}, \tag{C20}$$

is the same for all nodes $i \in \mathcal{N}_p$ and all cells $l, p = 1, ..., m_1$. Lemma 1 states that

$$\begin{aligned}\mathcal{V}_{\neq 0} &= \text{span}\left\{y_1, ..., y_{m_1}\right\} \\ &= \text{span}\left\{x_{\phi(1)}, ..., x_{\phi(m_1)}\right\}.\end{aligned}$$

Thus, there must be some nonsingular $m_1 \times m_1$ matrix H such that

$$\begin{pmatrix} x_{\phi(1)} & ... & x_{\phi(m_1)} \end{pmatrix} = \begin{pmatrix} y_1 & ... & y_{m_1} \end{pmatrix} H. \tag{C21}$$

Since the set eigenvectors x_i and the set of vectors y_l are orthonormal, the matrix H is orthogonal[8]. The eigendecomposition of the matrix B reads

$$\begin{aligned} B = &\begin{pmatrix} x_{\phi(1)} & ... & x_{\phi(m_1)} \end{pmatrix} \text{diag}\left(\lambda_{\phi(1)}, ..., \lambda_{\phi(m_1)}\right) \begin{pmatrix} x_{\phi(1)}^T \\ \vdots \\ x_{\phi(m_1)}^T \end{pmatrix} \\ &+ \begin{pmatrix} x_{\phi(m_1+1)} & ... & x_{\phi(m)} \end{pmatrix} \text{diag}\left(\lambda_{\phi(m_1+1)}, ..., \lambda_{\phi(m)}\right) \begin{pmatrix} x_{\phi(m_1+1)}^T \\ \vdots \\ x_{\phi(m)}^T \end{pmatrix} \\ &+ \begin{pmatrix} x_{\phi(m+1)} & ... & x_{\phi(N)} \end{pmatrix} \text{diag}\left(\lambda_{\phi(m+1)}, ..., \lambda_{\phi(N)}\right) \begin{pmatrix} x_{\phi(m+1)}^T \\ \vdots \\ x_{\phi(N)}^T \end{pmatrix}. \end{aligned}$$

With (C21), and since the eigenvalues $\lambda_{\phi(l)} = 0$ for $l = m_1 + 1, ..., m$, we obtain that

$$\begin{aligned} B = &\begin{pmatrix} y_1 & ... & y_{m_1} \end{pmatrix} H \,\text{diag}\left(\lambda_{\phi(1)}, ..., \lambda_{\phi(m_1)}\right) H^T \begin{pmatrix} y_1^T \\ \vdots \\ y_{m_1}^T \end{pmatrix} \\ &+ \begin{pmatrix} x_{\phi(m+1)} & ... & x_{\phi(N)} \end{pmatrix} \text{diag}\left(\lambda_{\phi(m+1)}, ..., \lambda_{\phi(N)}\right) \begin{pmatrix} x_{\phi(m+1)}^T \\ \vdots \\ x_{\phi(N)}^T \end{pmatrix}. \end{aligned} \tag{C22}$$

Consider two nodes $i \in \mathcal{N}_p$ and a subset $\mathcal{N}_l$ for some $l = 1, ..., m_1$. Since

$$(y_l)_j = \begin{cases} \frac{1}{\sqrt{|\mathcal{N}_l|}} & \text{if } j \in \mathcal{N}_l, \\ 0 & \text{if } j \notin \mathcal{N}_l, \end{cases}$$

we can express the sum (C20) as

$$\sum_{j \in \mathcal{N}_l} \beta_{ij} = \sqrt{|\mathcal{N}_l|} \begin{pmatrix} \beta_{i1} & ... & \beta_{iN} \end{pmatrix} y_l.$$

[8]Since $x_i^T x_j = 1$ if $i = j$ and $x_i^T x_j = 0$ if $i \neq j$ and analogously for the vectors y_i, y_j, it follows from $x_i^T x_j = y_i^T H^T H y_j$ that the matrix H is orthogonal.

Thus, with the $N \times 1$ basic vector e_i, it holds that

$$\sum_{j \in \mathcal{N}_l} \beta_{ij} = \sqrt{|\mathcal{N}_l|} e_i^T B y_l.$$

From the orthogonality of the vectors $y_1, ..., y_{m_1}$ and from $x_{\phi(k)}^T y_l = 0$ for $k = m+1, ..., N$, we obtain with (C22) that

$$\sum_{j \in \mathcal{N}_l} \beta_{ij} = \sqrt{|\mathcal{N}_l|} e_i^T \begin{pmatrix} y_1 & ... & y_{m_1} \end{pmatrix} H \operatorname{diag}\left(\lambda_{\phi(1)}, ..., \lambda_{\phi(m_1)}\right) H^T e_{m_1 \times 1, l}, \tag{C23}$$

where the l-th entry of the $m_1 \times 1$ vector $e_{m_1 \times 1, l}$ equals one, and the other entries of $e_{m_1 \times 1, l}$ equal zero. Since node i is element of exactly one subset $\mathcal{N}_p$, it holds that

$$e_i^T \begin{pmatrix} y_1 & ... & y_{m_1} \end{pmatrix} = \frac{1}{\sqrt{|\mathcal{N}_p|}} \tilde{e}_{m_1 \times 1, p}^T.$$

Then, (C23) becomes

$$\sum_{j \in \mathcal{N}_l} \beta_{ij} = d_{il},$$

where

$$d_{il} = \frac{\sqrt{|\mathcal{N}_l|}}{\sqrt{|\mathcal{N}_p|}} e_{m_1 \times 1, p}^T H \operatorname{diag}\left(\lambda_{\phi(1)}, ..., \lambda_{\phi(m_1)}\right) H^T e_{m_1 \times 1, l}$$

is the same for all nodes $i \in \mathcal{N}_p$, which completes the proof.

D Proof of Corollary 2

Since $R_0 > 1$, the viral state $v(t)$ converges to a positive steady state v_∞ as $t \to \infty$. Thus, the steady state v_∞ must be element of the $m = 1$ dimensional invariant set $\mathcal{V} = \operatorname{span}\{y_1\}$, which implies that $v_\infty = \tilde{c} y_1$ for some scalar c. Hence, the unit-length agitation mode equals either $y_1 = v_\infty / \|v_\infty\|_2$ or $y_1 = -v_\infty / \|v_\infty\|_2$. Without loss of generality assume that $y_1 = v_\infty / \|v_\infty\|_2$. Then, under Assumption 4, the matrix B is connected, which implies that $B y_1 \neq 0$ since the vector y_1 is positive. Thus, the subspace $\mathcal{V}_0$ must be empty.

To prove Corollary 2, we must show two directions. **"If" direction**: Suppose the infection rate matrix B is regular. Then, the viral state $v_{\infty,i}$ is the same for all nodes i, and $v(0) \in \mathcal{V}$ implies that $v_i(0) = v_j(0)$ for all nodes i, j. Since the matrix B is regular and the initial viral state $v_i(0)$ is the same for every node i, the approximation $v_{\text{apx}}(t) = c(t) v_\infty$ is exact [53, 42]. Since $v(t) = c(t) v_\infty$ at every time t, the invariant set $\mathcal{V} = \operatorname{span}\{y_1\}$ is indeed a one-dimensional invariant set of NIMFA.

"Only if" direction: Suppose the one-dimensional subspace $\mathcal{V} = \operatorname{span}\{y_1\}$ is an invariant set of NIMFA. Then, Theorem 2 yields that the infection rate matrix B has the equitable partition $\pi = \{\mathcal{N}_1\}$, where the cell $\mathcal{N}_1 = \{1, ..., N\}$ contains all nodes. Thus, (14) yields, that there exists some degree d_{11} which satisfies

$$\begin{aligned} d_{11} &= \sum_{k \in \mathcal{N}_1} \beta_{ik} \\ &= \sum_{k=1}^{N} \beta_{ik} \end{aligned}$$

for all nodes i. Thus, we obtain with definition (24) that the matrix B is regular.

E Proof of Theorem 3

By assumption, the infection rates $\beta_{i,j}$ are the same for all nodes i in any cell $\mathcal{N}_l$ and all nodes j in any cell $\mathcal{N}_p$. Thus, with the definition of the vectors y_1, ..., y_r in (23), the symmetric infection rate matrix equals

$$B = \begin{pmatrix} y_1 & ... & y_r \end{pmatrix} \tilde{B}_{\mathcal{V}_{\neq 0}} \begin{pmatrix} y_1^T \\ \vdots \\ y_r^T \end{pmatrix} \tag{E1}$$

for some symmetric $r \times r$ matrix $\tilde{B}_{\mathcal{V}_{\neq 0}}$. Since the kernel $\ker(B)$ is the orthogonal complement of the subspace $\mathcal{V}_{\neq 0}$, it holds that $\mathbb{R}^N = \mathcal{V}_{\neq 0} \oplus \ker(B)$. Thus, any viral state vector $v(t) \in [0,1]^N$ can be decomposed as $v(t) = \tilde{v}(t) + v_{\ker}(t)$, where $\tilde{v}(t) \in \mathcal{V}_{\neq 0}$ and $v_{\ker}(t) \in \ker(B)$. With the decomposition $v(t) = \tilde{v}(t) + v_{\ker}(t)$, NIMFA (2) becomes

$$\begin{aligned} \frac{dv(t)}{dt} &= -S\left(\tilde{v}(t) + v_{\ker}(t)\right) + \operatorname{diag}\left(u - \tilde{v}(t) - v_{\ker}(t)\right) B\left(\tilde{v}(t) + v_{\ker}(t)\right) \\ &= -S\tilde{v}(t) - Sv_{\ker}(t) + \operatorname{diag}\left(u - \tilde{v}(t) - v_{\ker}(t)\right) B\tilde{v}(t), \end{aligned}$$

where the second equality follows from $Bv_{\ker}(t) = 0$. Further rearrangement yields that

$$\frac{dv(t)}{dt} = (B - S)\,\tilde{v}(t) - \operatorname{diag}\left(\tilde{v}(t)\right) B\tilde{v}(t) - Sv_{\ker}(t) - \operatorname{diag}\left(v_{\ker}(t)\right) B\tilde{v}(t). \tag{E2}$$

We decompose the derivative $dv(t)/dt$ into two addends, by making use of two lemmas:

Lemma 6. *Suppose that the assumptions in Theorem 3 hold true. Then, if $\tilde{v} \in \mathcal{V}_{\neq 0}$, the vector*

$$B\tilde{v} - S\tilde{v} - \operatorname{diag}\left(\tilde{v}\right) B\tilde{v} \tag{E3}$$

is element of $\mathcal{V}_{\neq 0}$.

Proof. We consider the three addends of the vector (E3) separately. First, (E1) shows that the addend $B\tilde{v}$ is element of $\mathcal{V}_{\neq 0}$ if $\tilde{v} \in \mathcal{V}_{\neq 0}$. Second, we consider the addend $S\tilde{v}$. By assumption, the curing rates δ_i are the same for all nodes i in the same cell $\mathcal{N}_l$. Thus, we obtain from the definition of the agitation modes y_l in (23) that

$$Sy_l = \delta_i y_l \tag{E4}$$

for $l = 1, ..., r$, where i denotes an arbitrary node in cell $\mathcal{N}_l$. Since the agitation modes y_1, ..., y_r span the subspace $\mathcal{V}_{\neq 0}$, (E4) implies that $S\tilde{v}$ if $\tilde{v} \in \mathcal{V}_{\neq 0}$.

Third, we consider the addend $\operatorname{diag}\left(\tilde{v}\right) B\tilde{v}$. Since $\tilde{v} \in \mathcal{V}_{\neq 0}$, it holds that

$$\tilde{v} = \sum_{l=1}^{r} \left(y_l^T \tilde{v}\right) y_l.$$

Similarly, since $B\tilde{v} \in \mathcal{V}_{\neq 0}$, it holds that

$$B\tilde{v} = \sum_{l=1}^{r} \left(y_l^T B\tilde{v}\right) y_l. \tag{E5}$$

Thus, we obtain that

$$\operatorname{diag}(\tilde{v})\, B\tilde{v} = \sum_{l=1}^{r}\sum_{p=1}^{r} \left(y_l^T \tilde{v}\right)\left(y_p^T B\tilde{v}\right) \operatorname{diag}(y_l) y_p. \tag{E6}$$

From the definition of the vectors y_l in (23) it follows that

$$\operatorname{diag}(y_l)\, y_p = \begin{cases} y_l^2 & \text{if} \quad l = p, \\ 0 & \text{if} \quad l \neq p, \end{cases}$$

where the $N \times 1$ vector $y_l^2 = \left((y_l)_1^2, ..., (y_l)_N^2\right)^T$ denotes Hadamard product of the vector y_l with itself. Thus, (E6) becomes

$$\operatorname{diag}(\tilde{v})\, B\tilde{v} = \sum_{l=1}^{r} \left(y_l^T \tilde{v}\right)\left(y_l^T B\tilde{v}\right) y_l^2. \tag{E7}$$

With (23), the Hadamard product y_l^2 equals

$$(y_l)_i^2 = \begin{cases} \frac{1}{|\mathcal{N}_l|} & \text{if} \quad i \in \mathcal{N}_l, \\ 0 & \text{if} \quad i \notin \mathcal{N}_l, \end{cases}$$

which implies that $(y_l)^2 = y_l/\sqrt{|\mathcal{N}_l|}$ and yields with (E7) that

$$\operatorname{diag}(\tilde{v})\, B\tilde{v} = \sum_{l=1}^{r} \frac{\left(y_l^T \tilde{v}\right)\left(y_l^T B\tilde{v}\right)}{\sqrt{|\mathcal{N}_l|}} y_l.$$

Thus, the vector $\operatorname{diag}(\tilde{v})\, B\tilde{v}$ is a linear combination of the vectors y_1, ..., y_r, which implies that $\operatorname{diag}(\tilde{v})\, B\tilde{v} \mathcal{V}_{\neq 0}$. Hence, we have shown that all three addends of the vector (E3) are in $\mathcal{V}_{\neq 0}$, which completes the proof. □

Lemma 7. *Suppose that the assumptions in Theorem 3 hold true. Then, if* $\tilde{v} \in \mathcal{V}_{\neq 0}$ *and* $v_{\text{ker}} \in \ker(B)$*, the vector*

$$S v_{\text{ker}} + \operatorname{diag}(v_{\text{ker}})\, B\tilde{v} \tag{E8}$$

is element of $\ker(B)$*.*

Proof. The kernel $\ker(B)$ is the orthogonal complement of the subspace $\mathcal{V}_{\neq 0}$. Thus, the vector (E8) is element of $\ker(B)$ if $S v_{\text{ker}}$ is orthogonal to every basis vector y_1, ..., y_r of the subspace $\mathcal{V}_{\neq 0}$. We show separately that both addends of the vector (E8) are orthogonal to every vector y_1, ..., y_r. First, for any $l = 1, ..., r$, we obtain for the first addend in (E8) that

$$y_l^T S v_{\text{ker}} = (S y_l)^T v_{\text{ker}},$$

since the matrix S is symmetric. With (E4), we obtain for an arbitrary node $i \in \mathcal{N}_l$ that

$$y_l^T S v_{\text{ker}} = \delta_i y_l^T v_{\text{ker}} = 0.$$

Thus, the addend $S v_{\text{ker}}$ is element of $\ker(B)$.

Second, for any $l = 1, ..., r$, we obtain for the second addend in (E8) with (E5) that

$$\begin{aligned} y_l^T \operatorname{diag}(v_{\ker}) B\tilde{v} &= \sum_{q=1}^{r} \left(y_l^T B\tilde{v}\right) y_l^T \operatorname{diag}(v_{\ker}) y_q \\ &= \sum_{q=1}^{r} \left(y_q^T B\tilde{v}\right) v_{\ker}^T \operatorname{diag}(y_l) y_q. \end{aligned}$$

Analogous steps as in the proof of Lemma 6 yield that

$$y_l^T \operatorname{diag}(v_{\ker}) B\tilde{v} = \frac{\left(y_l^T B\tilde{v}\right)}{\sqrt{|\mathcal{N}_l|}} v_{\ker}^T y_l.$$

Thus, by the orthogonality of the vectors $v_{\ker}$ and y_l,

$$y_l^T \operatorname{diag}(v_{\ker}) B\tilde{v} = 0,$$

which completes the proof. □

With Lemma 6 and Lemma 7, we obtain from (E2) that

$$\frac{dv(t)}{dt} = \frac{d\tilde{v}(t)}{dt} + \frac{dv_{\ker}(t)}{dt},$$

where

$$\frac{d\tilde{v}(t)}{dt} = -S\tilde{v}(t) + \operatorname{diag}(u - \tilde{v}(t)) B\tilde{v}(t)$$

and

$$\frac{dv_{\ker}(t)}{dt} = -Sv_{\ker}(t) - \operatorname{diag}(v_{\ker}(t)) B\tilde{v}(t),$$

which completes the proof, since

$$\operatorname{diag}(v_{\ker}(t)) B\tilde{v}(t) = \operatorname{diag}(B\tilde{v}(t)) v_{\ker}(t).$$

F Proof of Theorem 4

Since the spreading rates are homogeneous, $\beta_{ij} = \beta$ and $\delta_i = \delta$ for all nodes i, j, the infection rate matrix equals

$$B = \beta u u^T, \tag{F1}$$

and the curing rate matrix equals

$$S = \delta I. \tag{F2}$$

Thus, with $r = 1$ cell $\mathcal{N}_1 = \{1, ..., N\}$, Theorem 3 yields that the viral state $v(t)$ can be decomposed as $v(t) = \tilde{v}(t) + v_{\ker}(t)$. We prove Theorem 4 in two steps. First, we show that the projection $\tilde{v}(t)$ equals $c_1(t)v_\infty$ at every time t. Second, we prove that the projection $v_{\ker}(t)$ equals $c_2(t)y_2$ at every time t.

F.1 Projection on the subspace $\mathcal{V}_{\neq 0}$

With the reduced-size curing rate matrix $S^\pi = \delta$ and the quotient matrix $B^\pi = N\beta$, Theorem 1 yields that the projection on the subspace $\mathcal{V}_{\neq 0}$ satisfies $\tilde{v}(t) = v^\pi(t)u$. The evolution (16) of the reduced-size, scalar viral state $v^\pi(t)$ becomes

$$\frac{dv^\pi(t)}{dt} = -\delta v^\pi(t) + (1 - v^\pi(t))\, N\beta v^\pi(t). \tag{F3}$$

We consider two cases for the value of the spreading parameters β and δ.

1. If $\delta \neq \beta N$, then the solution of (F3) equals [53]

$$v^\pi(t) = \frac{v^\pi_\infty}{2}\left(1 + \tanh\left(\frac{w}{2}t + \Upsilon_1(0)\right)\right)$$

with the reduced-size steady state $v^\pi_\infty = 1 - \frac{\delta}{\beta N}$, the viral slope $w = \beta N - \delta$ and the constant

$$\Upsilon_1(0) = \operatorname{arctanh}\left(2\frac{v(0)}{v^\pi_\infty} - 1\right).$$

Thus, the projection $\tilde{v}(t) = v^\pi(t)u$ is equal to $c_1(t)y_1$ at every time t.

2. If $\delta = \beta N$, then the differential equation (F3) reduces to

$$\frac{dv^\pi(t)}{dt} = -\delta\left(v^\pi(t)\right)^2,$$

whose solution equals

$$v^\pi(t) = \left(\delta t + \frac{1}{v^\pi(0)}\right)^{-1}.$$

With $v^\pi(0) = y_1^T v(0)/\sqrt{N}$, we arrive at the closed-form expression (30) for the function $c_1(t)$.

F.2 Projection on the kernel $\ker(B)$

With (F1) and (F2), Theorem 3 yields that the projection $v_{\ker}(t)$ obeys

$$\frac{dv_{\ker}(t)}{dt} = -\left(\delta I + \beta\, \operatorname{diag}\left(uu^T\tilde{v}(t)\right)\right) v_{\ker}(t).$$

Since $\tilde{v}(t) = c_1(t)y_1$ and $(y_1)_i = 1/\sqrt{N}$ for all nodes i, we obtain that

$$\begin{aligned}\frac{dv_{\ker}(t)}{dt} &= -\left(\delta I + \beta\sqrt{N}c_1(t)I\right) v_{\ker}(t)\\ &= -\left(\delta + \beta\sqrt{N}c_1(t)\right) v_{\ker}(t).\end{aligned} \tag{F4}$$

For any initial condition $v_{\ker}(0) \in \ker(B)$, the right side of (F4) is in the one-dimensional subspace $\operatorname{span}\{v_{\ker}(0)\}$. Thus, the projection $v_{\ker}(t)$ obeys $v_{\ker}(t) = c_2(t)v_{\ker}(0)$. We solve (F4) in two steps. First, we compute the initial condition $v_{\ker}(0)$. Since $v(0) = v_{\ker}(0) + c_1(0)y_1$, the initial condition $v_{\ker}(0)$ is obtained as

$$\begin{aligned}v_{\ker}(0) &= v(0) - c_1(0)y_1\\ &= v(0) - \left(y_1^T v(0)\right) y_1.\end{aligned}$$

Hence, it follows that

$$v_{\ker}(0) = \left(I - y_1 y_1^T\right) v(0).$$

Second, using $v_{\ker}(t) = c_2(t) v_{\ker}(0)$, we project (F4) on the initial condition $v_{\ker}(0)$ to obtain that the scalar function $c_2(t)$ obeys the linear differential equation

$$\frac{dc_2(t)}{dt} = -\delta c_2(t) - \beta\sqrt{N} c_1(t) c_2(t). \tag{F5}$$

Again, we consider two cases for the value of the spreading parameters β and δ.

1. If $\delta \neq \beta N$, then we obtain with the function $c_1(t)$ given by (27) that

$$\frac{dc_2(t)}{dt} = -\delta c_2(t) - \frac{w}{2}\left(1 + \tanh\left(\frac{w}{2}t + \Upsilon_1(0)\right)\right) c_2(t).$$

Hence, with the constant $\Phi = w/2 + \delta$, it follows that

$$\log\left(c_2(t)\right) = -\int_0^t \left(\Phi + \frac{w}{2}\tanh\left(\frac{w}{2}\xi + \Upsilon_1(0)\right)\right) d\xi.$$

The integral of the hyperbolic tangent equals to the logarithm of the hyperbolic cosine [2],

$$\int \tanh\left(\xi\right) d\xi = \log\left(\cosh(\xi)\right),$$

which yields that

$$\begin{aligned}\log\left(c_2(t)\right) &= -\Phi t - \frac{w}{2}\frac{2}{w}\log\left(\cosh\left(\frac{w}{2}t + \Upsilon_1(0)\right)\right) + K(0) \\ &= -\Phi t - \log\left(\cosh\left(\frac{w}{2}t + \Upsilon_1(0)\right)\right) + K(0)\end{aligned}$$

for some constant $K(0)$, which is equivalent to

$$\log\left(c_2(t)\right) = -\Phi t + \log\left(\cosh\left(\frac{w}{2}t + \Upsilon_1(0)\right)^{-1}\right) + K(0).$$

With the hyperbolic secant $\operatorname{sech}(x) = \cosh(x)^{-1}$, we obtain that

$$c_2(t) = \Upsilon_2(0) e^{-\Phi t} \operatorname{sech}\left(\frac{w}{2}t + \Upsilon_1(0)\right), \tag{F6}$$

where $\Upsilon_2(0) = \exp(K(0))$. At the initial time $t = 0$, (F6) becomes

$$c_2(0) = \Upsilon_2(0) \operatorname{sech}\left(\Upsilon_1(0)\right),$$

and it holds that

$$c_2(0) = \frac{v_{\ker}^T(0) v(0)}{\|v_{\ker}(0)\|_2^2}. \tag{F7}$$

Thus, with $\operatorname{sech}(x) = \cosh(x)^{-1}$, we obtain the constant $\Upsilon_2(0)$ as (29), which completes the proof.

2. If $\delta = \beta N$, then the function $c_1(t)$ is given by (30). Thus, the differential equation (F5) for the function $c_2(t)$ becomes

$$\frac{dc_2(t)}{dt} = -\delta c_2(t) - \beta N \left(\delta t + \frac{\sqrt{N}}{y_1^T v(0)}\right)^{-1} c_2(t).$$

Thus, it holds that

$$\log\left(c_2(t)\right) = -\int_0^t \delta + \beta N \left(\delta \xi + \frac{\sqrt{N}}{y_1^T v(0)}\right)^{-1} d\xi.$$

Since

$$\int \left(\delta \xi + \frac{\sqrt{N}}{y_1^T v(0)}\right)^{-1} d\xi = \frac{1}{\delta} \log\left(\delta \xi + \frac{\sqrt{N}}{y_1^T v(0)}\right),$$

we obtain for some constant $K_2(0)$ that

$$\begin{aligned}\log\left(c_2(t)\right) &= -\delta t - \frac{\beta N}{\delta} \log\left(\delta t + \frac{\sqrt{N}}{y_1^T v(0)}\right) + K_2(0) \\ &= -\delta t + \log\left(\left(\delta t + \frac{\sqrt{N}}{y_1^T v(0)}\right)^{-\frac{\beta N}{\delta}}\right) + K_2(0).\end{aligned}$$

Hence, the function $c_2(t)$ equals

$$c_2(t) = \tilde{\Upsilon}_2(0) e^{-\delta t} \left(\delta t + \frac{\sqrt{N}}{y_1^T v(0)}\right)^{-\frac{\beta N}{\delta}},$$

where $\tilde{\Upsilon}_2(0) = e^{K_2(0)}$. At the initial time $t = 0$, we obtain that

$$c_2(0) = \tilde{\Upsilon}_2(0) \left(\frac{\sqrt{N}}{y_1^T v(0)}\right)^{-\frac{\beta N}{\delta}}.$$

Thus, it holds that

$$\begin{aligned}\tilde{\Upsilon}_2(0) &= c_2(0) \left(\frac{\sqrt{N}}{y_1^T v(0)}\right)^{\frac{\beta N}{\delta}} \\ &= \frac{v_{\ker}^T(0) v(0)}{\|v_{\ker}(0)\|_2^2} \left(\frac{\sqrt{N}}{y_1^T v(0)}\right)^{\frac{\beta N}{\delta}},\end{aligned}$$

where the second equality follows from (F7).

G Proof of Theorem 5

The viral state $\tilde{v}_i(t)$ evolves as

$$\frac{d\tilde{v}_i(t)}{dt} = \tilde{f}_{\text{NIMFA},i}(\tilde{v}(t)),$$

where we define, for every node i,

$$\tilde{f}_{\text{NIMFA},i}(\tilde{v}(t)) = -\tilde{\delta}_i \tilde{v}_i(t) + (1 - \tilde{v}_i(t)) \sum_{j=1}^{N} \tilde{\beta}_{ij} \tilde{v}_j(t). \tag{G1}$$

Since $\tilde{\beta}_{ij} \geq \beta_{ij}$ and $\tilde{\delta}_i \leq \delta_i$ for all nodes i, we obtain an upper bound on NIMFA (1) as

$$\begin{aligned} \frac{dv_i(t)}{dt} &\leq -\tilde{\delta}_i v_i(t) + (1 - v_i(t)) \sum_{j=1}^{N} \tilde{\beta}_{ij} v_j(t) \\ &= \tilde{f}_{\text{NIMFA},i}(v(t)). \end{aligned}$$

Since $dv_i(t)/dt \leq \tilde{f}_{\text{NIMFA},i}(v(t))$, we can apply the *Kamke-Müller condition* [21, 30], see also [22]: If $v \leq \tilde{v}$ and $v_i = \tilde{v}_i$ implies that $\tilde{f}_{\text{NIMFA},i}(v) \leq \tilde{f}_{\text{NIMFA},i}(\tilde{v})$ for all nodes i, then $v(0) \leq \tilde{v}(0)$ implies that $v(t) \leq \tilde{v}(t)$ at every time $t \geq 0$.

Thus, it remains to show that $v \leq \tilde{v}$ and $v_i = \tilde{v}_i$ implies that $\tilde{f}_{\text{NIMFA},i}(v) \leq \tilde{f}_{\text{NIMFA},i}(\tilde{v})$. From (G1), we obtain that

$$\tilde{f}_{\text{NIMFA},i}(v) - \tilde{f}_{\text{NIMFA},i}(\tilde{v}) = -\tilde{\delta}_i (v_i - \tilde{v}_i) + (1 - v_i) \sum_{j=1}^{N} \tilde{\beta}_{ij} v_j - (1 - \tilde{v}_i) \sum_{j=1}^{N} \tilde{\beta}_{ij} \tilde{v}_j.$$

From $v_i = \tilde{v}_i$, it follows that

$$\tilde{f}_{\text{NIMFA},i}(v) - \tilde{f}_{\text{NIMFA},i}(\tilde{v}) = (1 - v_i) \sum_{j=1}^{N} \tilde{\beta}_{ij} v_j - (1 - v_i) \sum_{j=1}^{N} \tilde{\beta}_{ij} \tilde{v}_j,$$

which yields that

$$\begin{aligned} \tilde{f}_{\text{NIMFA},i}(v) - \tilde{f}_{\text{NIMFA},i}(\tilde{v}) &= \sum_{j=1}^{N} \tilde{\beta}_{ij} (v_j - v_i v_j - \tilde{v}_j + v_i \tilde{v}_j) \\ &= \sum_{j=1}^{N} \tilde{\beta}_{ij} (1 - v_i)(v_j - \tilde{v}_j). \end{aligned}$$

Since $(v_j - \tilde{v}_j) \leq 0$, we obtain that $\tilde{f}_{\text{NIMFA},i}(v) \leq \tilde{f}_{\text{NIMFA},i}(\tilde{v})$, which completes the proof.

H Proof of Theorem 6

Here, we prove that $v_i(t) \geq v_{\text{lb},l}(t)$ for all nodes i in any cell $\mathcal{N}_l$. The proof of $v_i(t) \leq v_{\text{ub},l}(t)$ follows analogously. First, we define the curing rates $\tilde{\delta}_{\max,i}$ by

$$\tilde{\delta}_{\max,i} = \delta_{\max,l}$$

for all nodes i in any cell $\mathcal{N}_p$. Thus, (33) implies that $\tilde{\delta}_{\max,i} \geq \delta_i$ for all nodes $i = 1, ..., N$.

Lemma 8. *For all nodes i, j, there are infection rates $\tilde{\beta}_{ij}$, which satisfy $\tilde{\beta}_{ij} \leq \beta_{ij}$ and*

$$\sum_{j \in \mathcal{N}_l} \tilde{\beta}_{ij} = d_{\min,pl} \tag{H1}$$

for all nodes i in any cell $\mathcal{N}_p$ and all cells $\mathcal{N}_l$.

Proof. With the definition of the lower bound $d_{\min,pl}$ in (31), we obtain that (H1) is satisfied if

$$\sum_{j\in\mathcal{N}_l} \tilde{\beta}_{ij} = \min_{i\in\mathcal{N}_p} \sum_{k\in\mathcal{N}_l} \beta_{ik}. \tag{H2}$$

Denote the difference of the infection rates by $\varepsilon_{ij} = \beta_{ij} - \tilde{\beta}_{ij}$. Thus, $\tilde{\beta}_{ij} \leq \beta_{ij}$ and $\tilde{\beta}_{ij} \geq 0$ holds if and only if $0 \leq \varepsilon_{ij} \leq \beta_{ij}$. We obtain from (H2) that the differences ε_{ij} must satisfy

$$\sum_{j\in\mathcal{N}_l} \beta_{ij} - \sum_{j\in\mathcal{N}_l} \varepsilon_{ij} = \min_{i\in\mathcal{N}_p} \sum_{k\in\mathcal{N}_l} \beta_{ik},$$

which yields that

$$\sum_{j\in\mathcal{N}_l} \varepsilon_{ij} = \sum_{j\in\mathcal{N}_l} \beta_{ij} - \min_{i\in\mathcal{N}_p} \sum_{k\in\mathcal{N}_l} \beta_{ik}. \tag{H3}$$

To complete the proof, we must show that there exist some $\varepsilon_{ij} \in [0, \beta_{ij}]$ that solve (H3). Since

$$\sum_{j\in\mathcal{N}_l} \beta_{ij} \geq \min_{i\in\mathcal{N}_p} \sum_{k\in\mathcal{N}_l} \beta_{ik}$$

and $\beta_{ij} \geq 0$, the right side of (H3) is some value in $[0, \sum_{j\in\mathcal{N}_l} \beta_{ij}]$. Since the feasible values of the infection rate differences ε_{ij} are in the interval $[0, \beta_{ij}]$, the left side of (H3) may attain an arbitrary value in $[0, \sum_{j\in\mathcal{N}_l} \beta_{ij}]$. Thus, there are some infection rate differences $\varepsilon_{ij} \in [0, \beta_{ij}]$ that solve (H3), which completes the proof. □

Lemma 8 states the existence of an $N \times N$ matrix $\tilde{B}_{\min}$ whose elements $\tilde{\beta}_{\min,ij}$ satisfy $\tilde{\beta}_{ij} \leq \beta_{ij}$ and (H1). Thus, π is an equitable partition of the matrix $\tilde{B}_{\min}$. We define the $N \times 1$ viral state $\tilde{v}_{\mathrm{lb}}(t)$ as

$$\frac{d\tilde{v}_{\mathrm{lb}}(t)}{dt} = -\operatorname{diag}\left(\tilde{\delta}_{\max,1}, ..., \tilde{\delta}_{\max,N}\right) \tilde{v}_{\mathrm{lb}}(t) + \operatorname{diag}\left(u - \tilde{v}_{\mathrm{lb}}(t)\right) \tilde{B}_{\min} \tilde{v}_{\mathrm{lb}}(t) \tag{H4}$$

with the initial viral state

$$\tilde{v}_{\mathrm{lb},i}(0) = \min_{j\in\mathcal{N}_p} v_j(0)$$

for all nodes i in any cell $\mathcal{N}_p$. Since $\tilde{v}_{\mathrm{lb},i}(0) \leq v_i(0)$, $\tilde{\delta}_{\max,i} \geq \delta_i$ and $\tilde{\beta}_{\min,ij} \leq \beta_{ij}$ for all nodes i, j, Theorem 5 yields that $\tilde{v}_{\mathrm{lb},i}(t) \leq v_i(t)$ for every node i at every time t. Furthermore, Theorem 1 yields that the N-dimensional dynamics of the viral state $\tilde{v}_{\mathrm{lb}}(t)$ in (H4) can be reduced to the r-dimensional dynamics of the reduced-size viral state $v_{\mathrm{lb}}(t)$ in (34), which completes the proof.